

SOLIDIFICATION OF THE HANFORD LAW WASTE STREAM PRODUCED AS A RESULT OF NEAR-TANK CONTINUOUS SLUDGE LEACHING AND SODIUM HYDROXIDE RECOVERY

J. R. Harbour
M.M. Reigel
F.C. Johnson
C. Crawford
C. Jantzen
K. Gustashaw

September 2011

Savannah River National Laboratory
Savannah River Nuclear Solutions
Aiken, SC 29808

**Prepared for the U.S. Department of Energy Under
Contract Number DE-AC09-08SR22470**



DISCLAIMER

This work was prepared under an agreement with and funded by the U.S. Government. Neither the U.S. Government or its employees, nor any of its contractors, subcontractors or their employees, makes any express or implied: 1. warranty or assumes any legal liability for the accuracy, completeness, or for the use or results of such use of any information, product, or process disclosed; or 2. representation that such use or results of such use would not infringe privately owned rights; or 3. endorsement or recommendation of any specifically identified commercial product, process, or service. Any views and opinions of authors expressed in this work do not necessarily state or reflect those of the United States Government, or its contractors, or subcontractors.

Printed in the United States of America

**Prepared For
U.S. Department of Energy**

REVIEWS AND APPROVALS

AUTHORS:

M.M. Reigel, SRNL, Engineering Process Development Date

F.C. Johnson, SRNL, Process Technology Programs Date

C. Crawford, SRNL, Process Technology Programs Date

C. Jantzen, SRNL, Process Technology Programs Date

TECHNICAL REVIEWERS:

A. D. Cozzi, SRNL, Engineering Process Development Date

APPROVERS

F. M. Pennebaker, SRNL, Manager, Advanced Characterization & Process Date

S. L. Marra, SRNL, Manager, E&CPT Research Programs Date

EXECUTIVE SUMMARY

The U.S. Department of Energy (DOE), Office of River Protection (ORP), is responsible for the remediation and stabilization of the Hanford Site tank farms, including 53 million gallons of highly radioactive mixed waste contained in 177 underground tanks.^{1,2} The plan calls for all waste retrieved from the tanks to be transferred to the Waste Treatment Plant (WTP). The WTP will consist of three primary facilities including pretreatment facilities for Low Activity Waste (LAW) to remove aluminum, chromium and other solids and radioisotopes that are undesirable in the High Level Waste (HLW) stream. Removal of aluminum from HLW sludge can be accomplished through continuous sludge leaching of the aluminum from the HLW sludge as sodium aluminate; however, this process will introduce a significant amount of sodium hydroxide into the waste stream and consequently will increase the volume of waste to be dispositioned. A sodium recovery process is needed to remove the sodium hydroxide and recycle it back to the aluminum dissolution process. The resulting LAW waste stream has a high concentration of aluminum and sodium and will require alternative immobilization methods.

Five waste forms were evaluated for immobilization of LAW at Hanford after the sodium recovery process. The waste forms considered for these two waste streams include low temperature processes (Saltstone/Cast stone and geopolymers), intermediate temperature processes (steam reforming and phosphate glasses) and high temperature processes (vitrification). These immobilization methods and the waste forms produced were evaluated for (1) compliance with the Performance Assessment (PA) requirements for disposal at the IDF, (2) waste form volume (waste loading), and (3) compatibility with the tank farms and systems.

The iron phosphate glasses tested using the product consistency test had normalized release rates lower than the waste form requirements although the CCC glasses had higher release rates than the quenched glasses. However, the waste form failed to meet the vapor hydration test criteria listed in the WTP contract. In addition, the waste loading in the phosphate glasses were not as high as other candidate waste forms. Vitrification of HLW waste as borosilicate glass is a proven process; however the HLW and LAW streams at Hanford can vary significantly from waste currently being immobilized. The CCC glasses show lower release rates for B and Na than the quenched glasses and all glasses meet the acceptance criterion of < 4 g/L. Glass samples spiked with Re_2O_7 also passed the PCT test. However, further vapor hydration testing must be performed since all the samples cracked and the test could not be performed. The waste loading of the iron phosphate and borosilicate glasses are approximately 20 and 25% respectively.

The steam reforming process produced the predicted waste form for both the high and low aluminate waste streams. The predicted waste loadings for the monolithic samples is approximately 39%, which is higher than the glass waste forms; however, at the time of this report, no monolithic samples were made and therefore compliance with the PA cannot be determined.

The waste loading in the geopolymer is approximately 40% but can vary with the sodium hydroxide content in the waste stream. Initial geopolymer mixes revealed compressive strengths that are greater than 500 psi for the low aluminate mixes and less than 500 psi for the high aluminate mixes. Further work testing needs to be performed to formulate a geopolymer waste form made using a high aluminate salt solution.

A cementitious waste form has the advantage that the process is performed at ambient conditions and is a proven process currently in use for LAW disposal. The Saltstone/Cast Stone formulated using low and high aluminate salt solutions retained at least 97% of the Re that was added to the mix as a dopant. While this data is promising, additional leaching testing must be performed to show compliance with the PA. Compressive strength tests must also be performed on the Cast Stone monoliths to verify PA compliance.

Based on testing performed for this report, the borosilicate glass and Cast Stone are the recommended waste forms for further testing. Both are proven technologies for radioactive waste disposal and the initial testing using simulated Hanford LAW waste shows compliance with the PA. Both are resistant to leaching and have greater than 25% waste loading.

TABLE OF CONTENTS

EXECUTIVE SUMMARY	IV
LIST OF FIGURES	VIII
LIST OF TABLES	IX
LIST OF ACRONYMS	X
1.0 INTRODUCTION AND BACKGROUND.....	11
2.0 CONTINUOUS SLUDGE LEACHING	12
2.1 Aluminum in Hanford Tanks.....	13
2.2 Aluminum Solubility	13
2.3 CSL Process	13
3.0 SODIUM RECOVERY PROCESSES	14
3.1.1 Ceramatec Process	15
3.1.2 Areva Process	16
3.2 Simulant Development	17
3.2.1 Ceramatec Simulant	17
3.2.2 Areva Simulant	21
4.0 IMMOBILIZATION WASTE FORMS	23
4.1 Iron phosphate Glass Waste Forms	23
4.1.1 Formulation	23
4.1.2 PCT	24
4.1.3 Vapor Hydration Test (VHT)	25
4.1.4 XRD	25
4.1.5 Volume and Mass Factors	28
4.2 Borosilicate Glass Waste Forms.....	28
4.2.1 Formulation	28
4.2.2 PCT	29
4.2.3 Vapor Hydration Tests	30
4.2.4 X-ray Diffraction	30
4.2.5 Volume and Mass Factors	32
4.2.6 Doped Glasses	32
4.3 Steam Reformed Waste Form	34
4.3.1 Formulation	35
4.3.2 BSR Equipment Setup	36
4.3.3 BSR Processing Conditions	38
4.3.4 XRD	39
4.3.5 Projected Waste Loadings	40
4.4 Geopolymer Waste Forms	40
4.4.1 Cementitious Materials and Simulants	41
4.4.2 Experimental Design and Batching	42
4.4.3 Measurement of Fresh and Cured Properties	43
4.4.4 Scanning Electron Microscopy	44
4.4.5 Heat Generation	49
4.4.6 Volume and Mass Factors	51
4.4.7 Future Work	52
4.5 Saltstone/Cast Stone Waste Form	52
4.5.1 Saltstone Formulation	52
4.5.2 Performance Properties of Saltstone	53
4.5.3 Radionuclide Retention	54
4.5.4 Future Work	56

5.0 CONCLUSIONS AND PATH FORWARD..... 57
6.0 ACKNOWLEDGEMENTS 58
7.0 REFERENCES 59

LIST OF FIGURES

Figure 1.1. Simplified Hanford Tank Waste Treatment and Immobilization Flow Diagram ²	11
Figure 2.1. Near Tank Treatment System Process Flow Diagram. ¹²	14
Figure 3.1. Schematic of an Electrochemical Process Using the NaSICON Membrane. ¹³	15
Figure 3.2. Schematic of WTP Process with the Areva LHT Process for Sodium Recovery. ¹⁹	16
Figure 3.3. Titration system showing alumina precipitation after all of the free hydroxide has been neutralized.	19
Figure 3.4. Results of titration of 50 mL of the low aluminate simulant precursor with 10 wt % nitric acid. The vertical lines identify the 200 mEq of free hydroxide and the total 250 mEq of hydroxide (includes 50 mEq of bound hydroxide) in the 50 mL of this simulant.....	19
Figure 3.5. Results of titration of 50 mL of the high aluminate simulant precursor with 10 wt % nitric acid. The vertical lines identify the 225 mEq of free hydroxide and the total 375 mEq of hydroxide (includes 150 mEq of bound hydroxide) in 50 mL of this simulant.	20
Figure 3.6. Lithium Hydrotalcite product after drying overnight at 60 °C	22
Figure 3.7. XRD pattern for LHT product.	23
Figure 4.1. Images of the VHT samples for (a) quenched MS-HAL-5, (b) ccc MS-HAL-5, (c) quenched MS-LAL-7 and (d) ccc MS-LAL-7.	25
Figure 4.2. XRD data for quenched MS-LAL-7 glass typical of an amorphous glass.	26
Figure 4.3. XRD data for ccc MS-LAL-7 glass showing at least two crystallites within the glass matrix.	26
Figure 4.4. XRD data for quenched MS-HAL-5 glass typical of an amorphous glass.	27
Figure 4.5. XRD data for ccc MS-HAL-5 glass showing approximately four crystalline phases within the glass matrix.	27
Figure 4.6. Images of the VHT samples for (a) quenched FCJHAL-1, (b) ccc FCJHAL-1, (c) quenched FCJLAL-3 and (d) ccc FCJLAL-3.	30
Figure 4.7. XRD spectra of the (a) quenched FCJLAL-3 glass, (b) FCJLAL-3ccc glass, (c) quenched FCJHAL-1 glass and (d) FCJHAL-1ccc.	31
Figure 4.8. Images of the VHT samples for (a) quenched FCJHAL-1D, (b) ccc FCJHAL-1D, (c) quenched FCJLAL-3D and (d) ccc FCJLAL-3D.	34
Figure 4.9. Na ₂ O-SiO ₂ -Al ₂ O ₃ ternary diagram showing the projected steam reformed waste form composition (blue square) for high and low aluminate waste streams.....	36
Figure 4.10. Schematic of the Bench-Scale Steam Reformer.	37
Figure 4.11. DMR chamber showing the 2.5 inch reaction zone. ²⁷	38
Figure 4.12. XRD plot of BSR product formulated with low aluminate simulant. Phases present are expected based on ternary phase diagram.	39
Figure 4.13. XRD plot of BSR product formulated with high aluminate simulant. Phases present are expected based on ternary phase diagram.	40
Figure 4.14. Low aluminate simulant and Big Brown Raw fly ash geopolymer paste after 14 days of curing at room temperature.	46
Figure 4.15. Low aluminate simulant mixed with big brown raw and slag geopolymer pastes after 14 days of curing at room temperature.	47
Figure 4.16. Low aluminate simulant mixed with Class C fly ash and slag geopolymer after 14 days of curing at room temperature	48
Figure 4.17. Low aluminate simulant mixed with Belews Creek fly ash and slag, geopolymer paste after 14 days of curing at room temperature.....	49
Figure 4.18. Isothermal calorimetry output for a mix of low aluminate waste stream # 1 with a premix composed of 85 wt % Big Brown Raw Class F fly ash and 15 wt % slag.	50
Figure 4.19. Isothermal calorimetry output for a mix of the low aluminate waste stream # 1 with a premix composed of 85 wt % Class C fly ash and 15 wt % slag.....	51

Figure 4.20. Normalized heat production (J/g of cm) for low and high aluminate mixes at 25 °C.	53
Figure 4.21. Dependence of Young’s modulus on the curing temperature of the grouts.	54
Figure 4.22. The UFA centrifuge system for measuring permeability and capturing pore solution.....	55
Figure 4.23. Total Na ion concentration (ppm) for each sample taken as a function of the total amount of solution collected.....	55

LIST OF TABLES

Table 3.1. Compositions of Precursors to the Low and High Aluminate Simulants	18
Table 3.2. Composition, Density and wt % Solids of the Low and High Aluminate Simulants.	21
Table 3.3. Solutions Used for Generating Lithium Hydrotalcite	22
Table 4.1. Target and Measured Glass Compositions for the HAL and LAL Iron Phosphate Glasses (wt%).....	24
Table 4.2. Normalized Concentrations for the HAL and LAL Phosphate Glasses.....	25
Table 4.3. Volume and Mass of Waste Form Produced per Liter of LAW with Phosphate Glass.....	28
Table 4.4. Target and Measured Glass Compositions for the HAL and LAL Borosilicate Glasses (wt%).....	29
Table 4.5. Normalized Concentrations for the HAL and LAL Borosilicate Glasses.....	29
Table 4.6. Summary of VHT Results for HAL and LAL Borosilicate Glasses.....	30
Table 4.7. Volume and Mass of Waste Form Produced per Liter of LAW with Borosilicate Glass.....	32
Table 4.8. Target and Measured Compositions for the Doped HAL and LAL Borosilicate Glasses (wt%).....	33
Table 4.9. Normalized Concentrations for the Doped HAL and LAL Borosilicate Glasses	33
Table 4.10. Re and I Leachate Results.....	34
Table 4.11. Summary of Corrosion Results for the Doped HAL and LAL Borosilicate Glasses.....	34
Table 4.12. Relative Scaling of Process Operating Parameters of the BSR Compared to the FBSR for the Hanford LAW simulants.	39
Table 4.13. Projected Waste Loadings for BSR Monolith Product.	40
Table 4.14. Oxide compositions of aluminosilicate powders based on Inductively Coupled Plasma-Emission Spectroscopy (ICP-ES).....	41
Table 4.15. Chemical Constituents and Concentrations of Simulants.	42
Table 4.16. Test Matrix for Geopolymer Mixtures with the Low Aluminate Waste Stream 1.	43
Table 4.17. Gel time, normalized bleed water and compressive strength for all geopolymer mixtures tested.	44
Table 4.18. Volume and mass fractions of geopolymer waste form.....	51
Table 4.19 Cementitious Materials Used in Saltstone/Cast Stone Waste Form.	52
Table 4.20. Processing properties for simulated low and high aluminate waste streams.	53
Table 4.21. Re Retention in the Low and High Aluminate Mixes.....	56
Table 4.22. Waste Loadings and Associated Volume and Mass Factors for the Mixes.	56

LIST OF ACRONYMS

ACTL	Aiken County Technology Laboratory
ASTM	American Society for Testing and Materials
BFS	Blast Furnace Slag
CBO	Carbon Burn-Out
CCC	Canister Center-Line Cooled
CM	Cementitious Materials
CSH	Calcium Silicate Hydrate
CSL	Continuous Sludge Leaching
DMR	De-nitration Mineralization Reactor
DOE	Department of Energy
BSR	Bench Scale Steam Reformer
DSS	Decontaminated Salt Solution
E	Dynamic Young's Modulus
EM	Environmental Management
FA	Class F Fly Ash
FBSR	Fluidized Bed Steam Reforming
HAL	High Aluminate
HLW	High Level Waste
ICP	Inductively Coupled Plasma
IDF	Integrated Disposal Facility
LAW	Low Activity Waste
LAL	Low Aluminate
LHT	Lithium Hydrotalcite
MCU	Modular Caustic Side Solvent Extraction
NaSICON	Sodium (Na) Super Ion Conductor
NRC	Nuclear Regulatory Commission
NTTS	Near-Tank Treatment System
ORP	Office of River Protection
PA	Performance Assessment
PC	Portland Cement
PCT	Product Consistency Test
PEP	Pretreatment Engineering Platform
PNNL	Pacific Northwest National Laboratory
SEM	Scanning Electron Microscopy
SPF	Saltstone Production Facility
SRNL	Savannah River National Laboratory
SRNS	Savannah River Nuclear Solutions
SRS	Savannah River Site
UFA	Unsaturated Flow Apparatus
VHT	Vapor Hydration Test
w/cm	Water to Cementitious Material Ratio
WTP	Waste Treatment and Immobilization Plant
XRD	X-ray Diffraction

1.0 Introduction and Background

The U.S. Department of Energy (DOE), Office of River Protection (ORP), is responsible for the remediation and stabilization of the Hanford Site tank farms, including 53 million gallons of highly radioactive mixed waste contained in 177 underground tanks.^{1,2} The plan calls for all waste retrieved from the tanks to be transferred to the Waste Treatment Plant (WTP). The WTP will consist of three primary facilities: a pretreatment facility and two facilities for Low Activity Waste (LAW) and HLW vitrification (Figure 1.1). The pretreatment facility will receive waste feed from the Hanford tank farms and separate it into two treated process streams: a high-volume, low-activity, liquid process stream stripped of most solids and high-activity radioisotopes and a much smaller volume HLW slurry containing most of the solids, high-activity radioisotopes, and long-lived isotopes. In the pretreatment facility, solids and radioisotopes will be removed from the tank waste by precipitation, filtrations, and ion exchange processes to produce the LAW streams. The slurry of filtered solids will be blended with two ion exchange streams containing soluble radioisotopes to produce the HLW streams. The primary constituents that will be removed from the HLW prior to receipt at the WTP are aluminum (boehmite) and phosphate wastes. Treatment of boehmite will dramatically reduce the process cycle time for the WTP pretreatment facility while treatment of the phosphate will significantly reduce the volume of material processed by the ion exchange columns in WTP. The pretreated HLW mixture will route to the HLW Vitrification Facility and the pretreated LAW stream will route to the LAW Vitrification Facility. These two vitrification facilities will convert these process streams into glass, which is poured directly into stainless steel canisters.

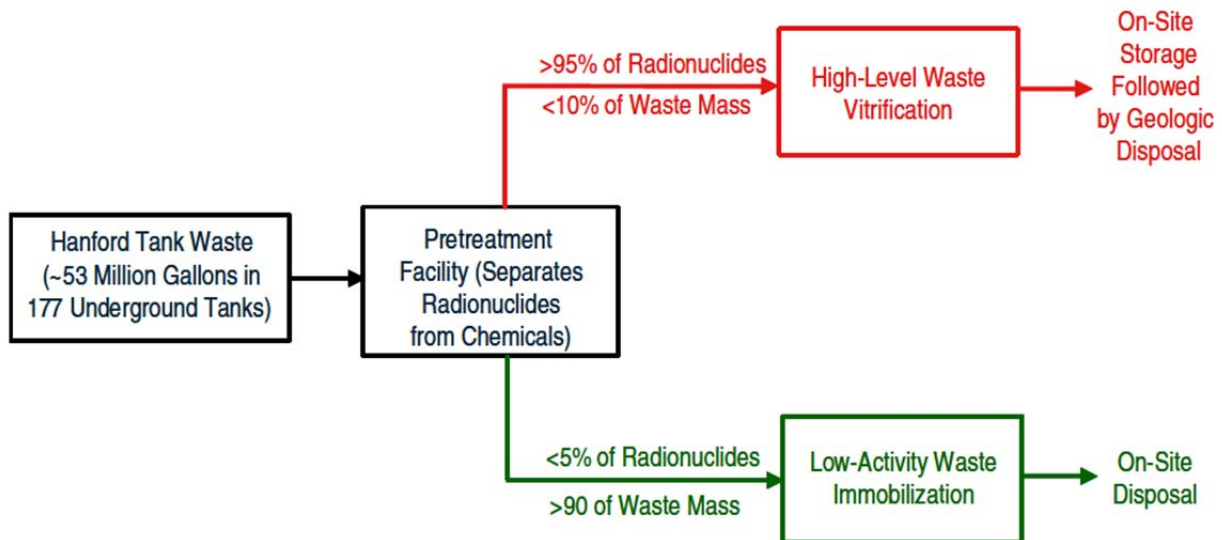


Figure 1.1. Simplified Hanford Tank Waste Treatment and Immobilization Flow Diagram²

Removal of aluminum from High Level Waste (HLW) sludge can be accomplished through caustic (NaOH) leaching of the aluminum from the HLW sludge as sodium aluminate, $\text{Na}^+\text{Al}(\text{OH})_4^-$. A continuous process has been developed to perform this aluminum leaching step for near tank applications at the Hanford Site. However, this process will introduce a significant amount of sodium hydroxide into the waste stream and consequently will increase the volume of waste to be dispositioned. In order to reduce this sodium load, a second process was introduced to remove the sodium hydroxide and recycle it back to the aluminum dissolution process.³

The rationale for this at or near tank waste treatment approach is to (1) reduce the volume of vitrified HLW produced over the lifetime of WTP and (2) facilitate the early treatment of some of the HLW waste prior to the startup of the WTP. This will generate a waste stream prior to startup of WTP that will be immobilized for disposal as LAW at the Integrated Disposal Facility (IDF) at Hanford. This report will consider various methods of immobilization for the LAW waste stream to produce a waste form that meets the requirements of the IDF, produces an acceptable waste volume, and can be implemented at or near tank. Near Tank Cesium Removal (NTCR) will also be integrated into this system as necessary to ensure the reduction of the LAW to a Nuclear Regulatory Commission (NRC) Class C limits as defined by CFR 61.55.³

One of the sodium recovery processes considered was developed by Ceramatec and involves an electrochemical driven transfer of sodium through a ceramic membrane. The overall result of this process is transfer of NaOH from the caustic, aluminum-rich waste stream in the anode cell to an aqueous solution in the cathode cell. This sodium recovery process can concentrate NaOH to 19 M in the cathodic stream. It is this concentrated NaOH solution that will be recycled to the continuous sludge leaching process. An important issue with this process is the formation of a waste stream either close to saturation or at a state of super-saturation in aluminate. Consequently, alumina can precipitate out of solution and generate a slurry of alumina in salt solution as the LAW stream to be treated. The formation of this precipitate in the waste stream depends on the chemistry of the initial stream and the degree to which the NaOH removal is performed. Therefore, a wastes immobilization option must consider the physical and chemical nature of the slurry for both processing and immobilization.³

A second process being considered for sodium recovery uses lithium hydroxide to precipitate out crystalline lithium hydroxalite (LHT) particles (as well as other mineral hydroxalites). The particle size of the LHT is typically on the order of 50 microns. These particles can then be filtered leaving a NaOH supernate that will be recycled to continuous aluminum dissolution process. The filtered LHT particles may be washed to reduce the amount of radionuclides in the waste stream to an acceptable level. This process therefore, produces a slurry of LHT particles in a salt solution. As with the Ceramatec process, this LHT waste immobilization option must consider the physical and chemical nature of the slurry for both processing and ultimate immobilization.³

Methods of immobilization that will be considered for these two waste streams include low temperature processes (Saltstone/Cast stone and geopolymers), intermediate temperature processes (steam reforming and phosphate glasses) and high temperature processes (vitrification). These immobilization methods and the waste forms they produce will be evaluated for (1) compliance with the Performance Assessment (PA) requirements for disposal at the IDF, (2) waste form volume (waste loading), and (3) compatibility with the tank farms and systems.³

2.0 Continuous Sludge Leaching

The Continuous Sludge Leaching (CSL) Process is being developed under EM's Advanced Remediation Technology (ART) Program by Parsons Infrastructure & Technology Group and the Pacific Northwest National Laboratory (PNNL) to remove aluminum and other undesirable compounds, such as chromium, from Hanford HLW. The WTP has a processing target to remove significant aluminum such that it is no longer the waste-limiting component in the final HLW glass waste form.⁴ The chromium must also be removed before producing the glass waste forms because there is low tolerance for it in the immobilization process due to chromium's low solubility in borosilicate waste glass.

2.1 Aluminum in Hanford Tanks

Aluminum present in the HLW tanks at Hanford, if not removed, would substantially increase the number of vitrified HLW waste canisters sent to a geologic waste repository since it is a waste-limiting component in the HLW glass form.^{2,4} The most abundant elements in the tanks include iron, phosphorous, calcium, silicon, bismuth and aluminum, which is one of the most prevalent, accounting for nearly 70% of the sludge.⁵ Aluminum is primarily found in the forms of gibbsite, $Al(OH)_3$, as micrometer sized colloidal particles or boehmite, $AlO(OH)$, as agglomerated nanoparticles⁵; however, there are a large number of other aluminum compounds present (sodium aluminate), including some compounds (e.g., refractory aluminosilicates) that are resistant to leaching.² The fundamental problem, from a chemistry perspective, is the wastes largely begin as gibbsite, but gradually convert to boehmite or other mineral forms as the wastes age.

2.2 Aluminum Solubility

Many studies have been performed that demonstrate the aluminum solubility in sodium hydroxide solutions depends on the mineral form of aluminum.⁷ As mentioned in the previous section, the most prevalent aluminum-containing minerals in Hanford tanks are gibbsite and boehmite;⁸ however, the dominant aluminum species in high-pH liquids is thought to be the aluminate ion $Al(OH)_4^-$. Gibbsite and sodium aluminate are easily dissolved by heating under caustic conditions (i.e. 8 hours at 50 °C with 3 M NaOH).⁸ The reaction between free hydroxide, aluminate and gibbsite is shown in Equation 1. Sodium aluminate forms according to Equation 2.



According to Equations 2.1 and 2.2, adding free hydroxide dissolves gibbsite and adding sodium allows sodium aluminate to precipitate. Thus, when sodium hydroxide is added to a solution with solid gibbsite, the gibbsite dissolves. If enough sodium hydroxide is added, sodium aluminate will re-precipitate. Therefore, there is an optimal sodium hydroxide concentration where the maximum quantity of aluminum (gibbsite) is dissolved while avoiding sodium aluminate precipitation.⁸

Multiple studies have been conducted on the dissolution kinetics of boehmite in caustic solutions.^{4,6,8} These studies have shown that the dissolution rate of boehmite is the rate-limiting step in aluminum dissolution and sensitive to temperature changes. One study showed the dissolution rate approximately doubles with every 20 °C temperature increase.⁸ Boehmite dissolution (Equation 2.3) requires more aggressive conditions of higher temperatures and longer time than to dissolve gibbsite.⁴ Both the precipitation and dissolution kinetics of boehmite are extremely slow at current tank temperatures.^{8,9}



According to waste dissolution studies on batch processes,^{4,6,8} the adequate dissolution of boehmite from Hanford tank waste can be achieved in approximately 24 hours using a 3 – 5 M NaOH solution at 100 °C.

2.3 CSL Process

The process uses a continuously stirred reactor vessel operating with caustic at 90 to 100 °C to remove aluminum and chromium by leaching with NaOH (Figure 2.1). The potential advantages of this approach are that it uses a longer residence time with a smaller footprint than the current semi-batch WTP pretreatment process based on reactor configuration to facilitate more complete aluminum extraction and may be applied in a near-tank configuration.² The extended residence time and higher temperature allow

for an increase in boehmite dissolution and reduced HLW canister production. Implementation of CSL could reduce the amount of Al and Cr in HLW by more than a factor of 2 by removing 90% of the boehmite. Currently, the WTP flow sheet targets less than 50% of the boehmite for dissolution.¹⁰ Deployment of the CSL process could result in approximately one third to one half reduction in the quantity of HLW canisters produced at Hanford, which results in up to \$10 billion in life cycle savings.¹¹

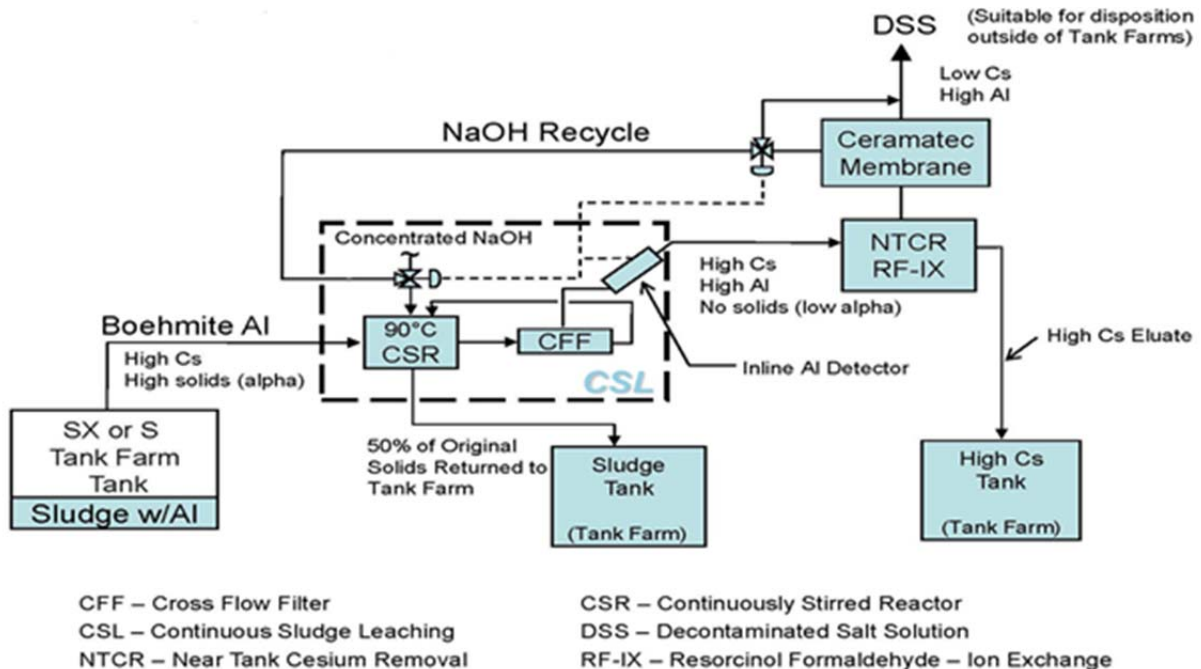


Figure 2.1. Near Tank Treatment System Process Flow Diagram.¹²

The full scale process will include a 3000 gallon reactor vessel and approximately 100 square feet of filter area (100 tube bundle).¹⁰ The CSL process will be designed to process 200 kg/hr of waste, produce 150 kg/hr of leached slurry, remove 90% of aluminum and reduce the mass of insoluble solids by 60%.¹⁰ A benefit of CSL implementation at Hanford is that it does not introduce any new hazards to the site since it utilizes existing chemicals, reduces the quantity of material at risk relative to the process baseline and the small reactor size reduces potential doses to workers.¹¹ However, removal of aluminum from HLW results in a substantial increase in the amount of sodium to be processed in LAW because of the addition of sodium hydroxide to increase aluminum solubility and prevent corrosion.²

3.0 Sodium Recovery Processes

Dissolving or leaching aluminum from Hanford tank sludges and maintaining its solubility during pretreatment requires the addition of large amounts of sodium hydroxide.⁹ Recent projections at Hanford indicate that up to 40,000 metric tons of sodium would be needed to dissolve the aluminum and maintain it in solutions, which nearly doubles the amount of sodium in the entire current waste tank inventory.⁶ Therefore, a sodium recovery process must be implemented that allows the caustic to be recycled through the CSL process to minimize the amount of required caustic.

3.1.1 Ceramatec Process

The first option for sodium recovery after CSL, developed by Ceramatec, electrochemically transfers sodium ions through a Sodium (Na) Super Ion Conductor (NaSICON) ceramic membrane while generating free hydroxide ions and hydrogen at the cathode and oxygen and hydrogen ions at the anode.¹³⁻¹⁵ This process shows promise as a means to mitigate the impact of Na by enabling the separation and recycling of Na from the radioactive wastes. In this process, the waste is added to the anode compartment, and an electrical potential is applied to the cell. The ceramic membrane allows the selective transport of Na⁺ ions to the cathode compartment while most other cations (e.g., K⁺, Cs⁺) and anions are left behind (i.e., rejected) in the anode compartment. The charge balance in the anode compartment is maintained by generating H⁺ from the electrolysis of water. The charge balance in the cathode is maintained by generating OH⁻, either from the electrolysis of water or from oxygen and water using an oxygen gas diffusion cathode.¹³ The normal gaseous products of the electrolysis of water are oxygen at the anode and hydrogen at the cathode. Potentially flammable gas mixtures can be prevented by providing adequate volumes of a sweep gas, using an alternative reductant, or destroying the hydrogen as it is generated. As H⁺ is generated in the anode compartment the pH drops and the waste stream becomes less alkaline.^{13,15} Producing OH⁻ in the cathode compartment results in a rise in pH as the Na hydroxide product is produced.¹³ Figure 3.1 is a schematic of the electrochemical process using the NaSICON membrane.

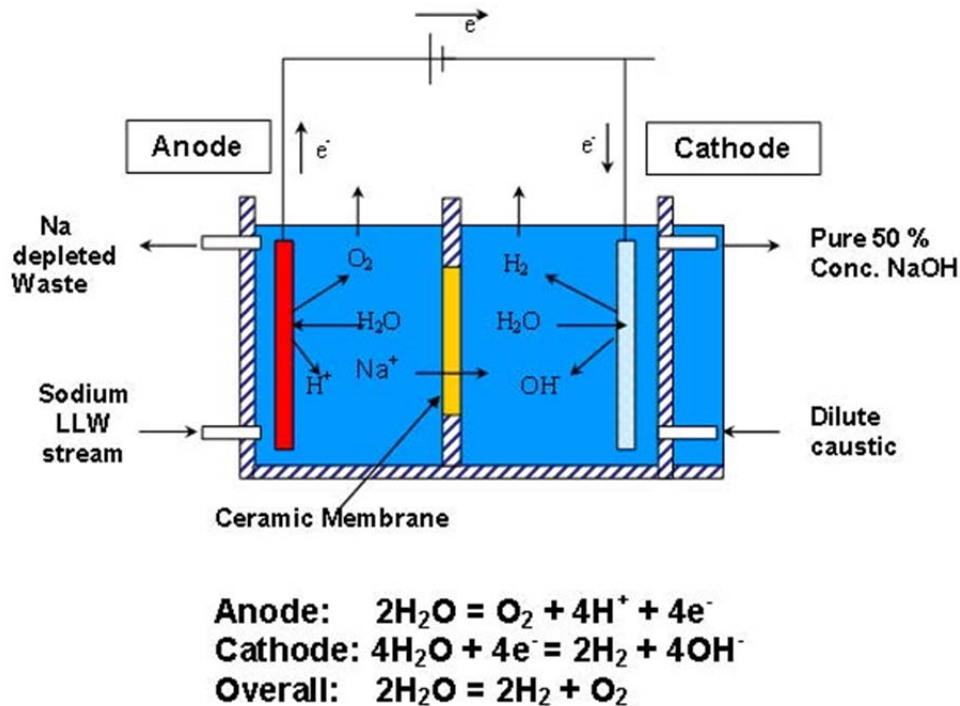


Figure 3.1. Schematic of an Electrochemical Process Using the NaSICON Membrane.¹³

The overall result of this process is transfer of NaOH from the caustic, aluminum-rich waste stream in the anode cell to an aqueous solution in the cathode cell. This sodium recovery process can concentrate NaOH to 19 M in the cathodic stream. It is this concentrated NaOH solution that will be recycled to the continuous sludge leaching process. An important issue with this process is the formation of a waste stream either close to saturation or at a state of super-saturation in aluminate. Consequently, alumina can precipitate out of solution and generate a slurry of alumina in salt solution as the LAW stream to be treated. The formation of this precipitate in the waste stream depends on the chemistry of the initial stream and the degree to which the NaOH removal is performed. Therefore, a waste immobilization

option must consider the physical and chemical nature of the slurry for both processing and immobilization.³

There are multiple benefits to this technology including a reduction in handling and processing of waste and potential cost savings for waste cleanup by lowering the volume of waste processed.¹⁶ The concentrated NaOH solution generated at the anode is recycled for continued aluminum leaching of the HLW sludge. The NaSICON ceramic membrane technology will directly make sodium hydroxide up to 50 wt% and prevents migration of cesium and other radionuclides to the sodium hydroxide stream.¹⁶

3.1.2 Areva Process

The second option for sodium recovery, developed by AREVA, adds lithium hydroxide to the waste stream to precipitate the leached aluminum as a lithium hydrotalcite (LHT) (Figure 3.2).^{14,17} The proposed LHT process theoretically eliminates the large volume of additional sodium hydroxide required to leach and maintain alumina solubility through Hanford Waste Treatment Plant (WTP) operations.¹⁸

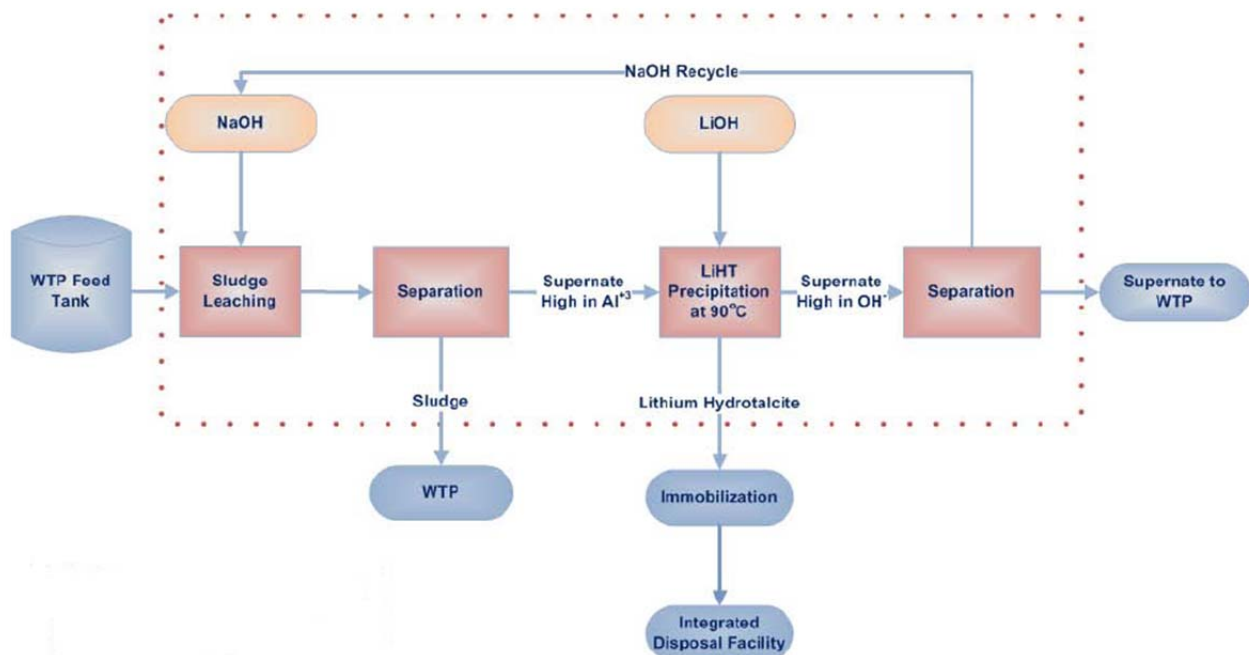
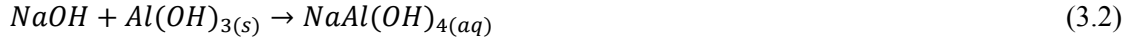


Figure 3.2. Schematic of WTP Process with the Areva LHT Process for Sodium Recovery.¹⁹

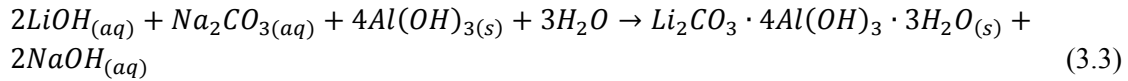
The key reaction in Equation 3.1.¹⁸ A 10% aqueous solution of lithium hydroxide (LiOH) is reacted with soluble sodium aluminate (NaAl(OH)_4) and sodium carbonate* (Na_2CO_3) present in the waste to produce lithium hydrotalcite ($\text{Li}_2\text{CO}_3 \cdot 4\text{Al(OH)}_3 \cdot 3\text{H}_2\text{O}$) and sodium hydroxide (NaOH). The solid lithium hydrotalcite is separated from solution; the aqueous sodium hydroxide is recycled to further leach alumina sludge as shown in Equation 3.2.¹⁸

(3.1)

* Aqueous sodium carbonate ($\text{Na}_2\text{CO}_{3(\text{AQ})}$) is abundant in Hanford waste. In the absence of sodium carbonate, another abundant sodium salt (e.g. $\text{NaNO}_{3(\text{AQ})}$) may substitute.



The combination of alumina sludge leaching (3.1) and lithium hydrotalcite precipitation (3.2) continuously liberates sodium hydroxide that can be recycled to the waste while removing alumina as a filterable solid (Equation 3.3).¹⁸



Analytical results of the experiments concur with literature reports and thermodynamic models of the method. The hydrotalcite reaction (3.1) occurs rapidly at 90°C. Thermodynamic studies indicate that reaction yield is maximized at low temperature (25°C). However, at this temperature the kinetic rate of reaction is slow and will require a large vessel to provide long residence time. Work is being performed to determine the optimum reaction temperature to achieve a balance between product yield and reaction rate.¹⁸

To improve the efficiency of LHT alumina removal, the leachate should be saturated or near-saturated in alumina. By this method, the maximum amount of alumina is leached and precipitated per gallon of solution. However, leaching rate decreases asymptotically as saturation is reached, and the required residence time to reach full saturation increases exponentially. Thus, a practical limit to the approach to alumina saturation will be determined.¹⁸ The product forms large (50 µm) particles with narrow size distribution, and can be separated and decontaminated from simulated waste solution easier than other precipitated alumina phases.¹⁸ A non-radioactive cesium decontamination factor (¹³⁴Cs DF) of >2,000 was obtained by water washing of the filter cake. Product purity was >99.9%. Theoretical yield (95%) was obtained in less than one-half hour of reaction time. Sodium hydroxide was regenerated by the reaction and recycled for alumina leaching.¹⁸ The filtered and washed LHT particles will then be immobilized for disposal at IDF. The concentrated filtrate, high in NaOH concentration, will be recycled for continued HLW sludge leaching.

Theoretically, this method can eliminate the large sodium hydroxide demand to leach alumina sludge and reduce two-thirds⁴ of the total sludge mass to be treated by the WTP. The actual amount of sodium hydroxide savings and alumina sludge reduction will depend upon the success of the development, the extent of implementation of the technology, and the amount of waste treated by this method.¹⁸

3.2 Simulant Development

Since the CSL and sodium hydroxide recovery processes are developmental, the first step in the task of waste form development is to produce model simulants to initiate evaluation of various immobilization methods. The simulants are based on the potential implementation of a Near-Tank Treatment System (NTTS) consisting of CSL of HLW followed by cesium-137 removal through ion exchange and sodium hydroxide recovery.¹⁴ It is assumed that cesium removal through ion exchange will not significantly change the chemical composition of the waste stream solution. As additional results are obtained from the CSL and sodium recovery processes, the simulant compositions will be refined. In addition, simulants will also be developed that bracket the compositional ranges due to projected variations in these processes.¹⁴ Although the Areva simulant was developed for testing with the candidate waste forms, the scope of the project was altered during the testing phase of this project and therefore the waste forms were formulated using the high and low aluminate solution simulants from the Ceramatec process only.

3.2.1 Ceramatec Simulant

Two simulants were prepared for the processes involving CSL followed by the Ceramatec sodium recovery process. The low aluminate simulant is based on a demonstration of the CSL process.²⁰ The

high aluminate simulant was based on the PEP simulant and analytical results during PEP pilot scale testing. Ceramatec tested both of these aluminum-leached simulants at their Salt Lake City facility using this sodium recovery process. The measured NaOH and aluminate concentrations prior to and after sodium recovery were used in this simulant development.¹⁴ The goal of this sodium recovery process is to recover as much NaOH as possible for recycle without producing an aluminum hydroxide precipitate in the waste stream. The presence of aluminum precipitates would produce a stream that could easily foul the downstream processes. Secondly, the recycling of NaOH reduces the amount of sodium in the LAW stream and consequently the volume of LAW waste form produced.¹⁴

In order to produce simulants that remain in solution, precursor simulants were batched with compositions based on the waste streams after aluminum dissolution but before sodium recovery. These precursor simulants were then titrated with nitric acid to determine the point where irreversible precipitation of aluminum hydroxide occurs. This titration simulates the removal of NaOH by the Ceramatec electrochemical process. Once this point is determined, the next step was to provide a safety margin in hydroxide ion concentration to prevent precipitation. The compositions of the precursors to the low and high aluminate simulants (prior to sodium recovery) are provided in Table 3.1. The titration system is shown in Figure 3.3. This photograph shows an injection of the nitric acid and formation of the alumina precipitate after all of the free hydroxide ions had been neutralized.¹⁴

Table 3.1. Compositions of Precursors to the Low and High Aluminate Simulants

Compound	Precursor Simulants	
	Low Aluminate (M)	High Aluminate (M)
NaOH	5.000	7.500
NaNO ₃	0.147	0.160
NaNO ₂	0.054	0.005
Na ₂ CO ₃	0.055	0.055
Na ₂ C ₂ O ₄	0.001	0.001
Na ₂ SO ₄	0.001	0.018
Al(NO ₃) ₃	0.250	0.750
Na ₃ (PO ₄)	0.002	0.000
Total Na Molarity	5.32	7.81



Figure 3.3. Titration system showing alumina precipitation after all of the free hydroxide has been neutralized.

Titration results for the low aluminate simulant precursor are provided in Figure 3.4. In this test, 50 mL of the simulant were titrated with a 10 wt % nitric acid solution. There are 200 mEq of free hydroxide ions and 50 mEq of bound hydroxide ions associated with $\text{Al}(\text{OH})_4^-$ (and 2.8 mEq from the carbonate and oxalate) in 50 mL of this simulant precursor.

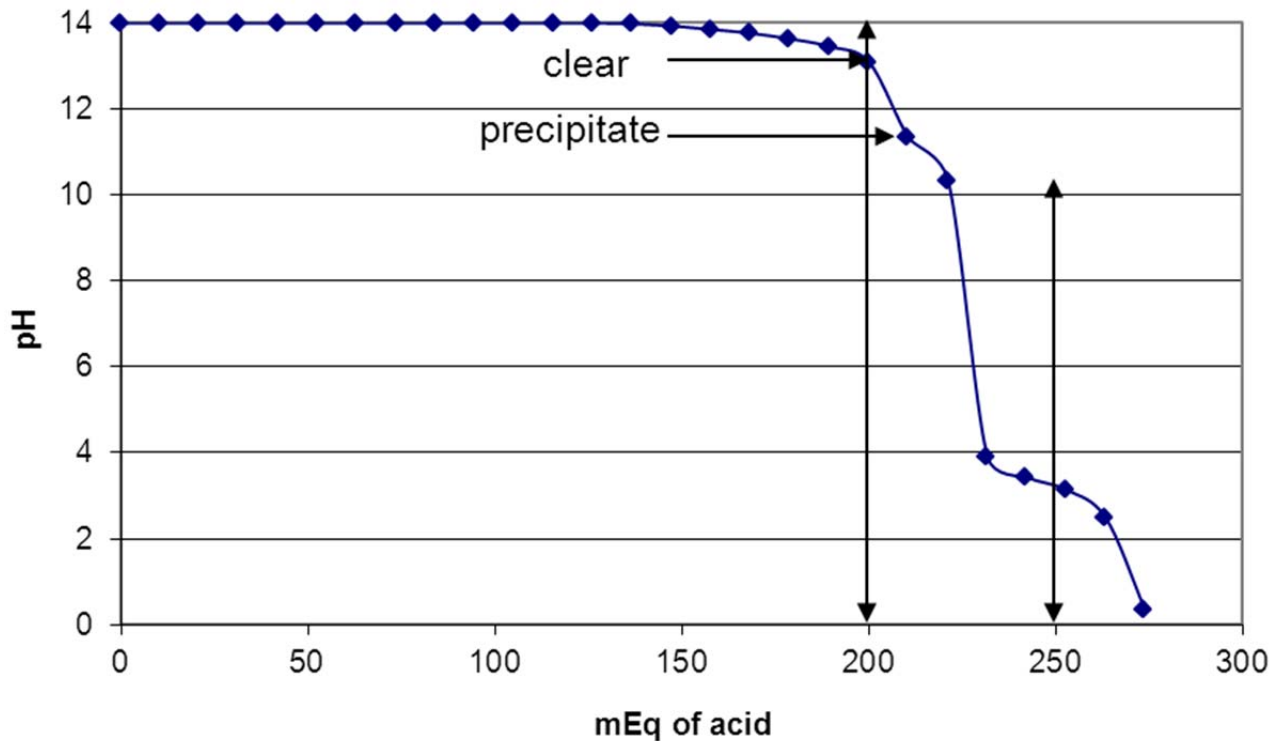


Figure 3.4. Results of titration of 50 mL of the low aluminate simulant precursor with 10 wt % nitric acid. The vertical lines identify the 200 mEq of free hydroxide and the total 250 mEq of hydroxide (includes 50 mEq of bound hydroxide) in the 50 mL of this simulant.

Titration results for the high aluminate simulant precursor are provided in Figure 3.5. In this test, 50 mL of the simulant were titrated with 10 wt % nitric acid. There are 225 mEq of free hydroxide ions and 150 mEq of bound hydroxide ions associated with $\text{Al}(\text{OH})_4^-$ (and 2.8 mEq from carbonate and oxalate) in 50 mL of this simulant precursor.

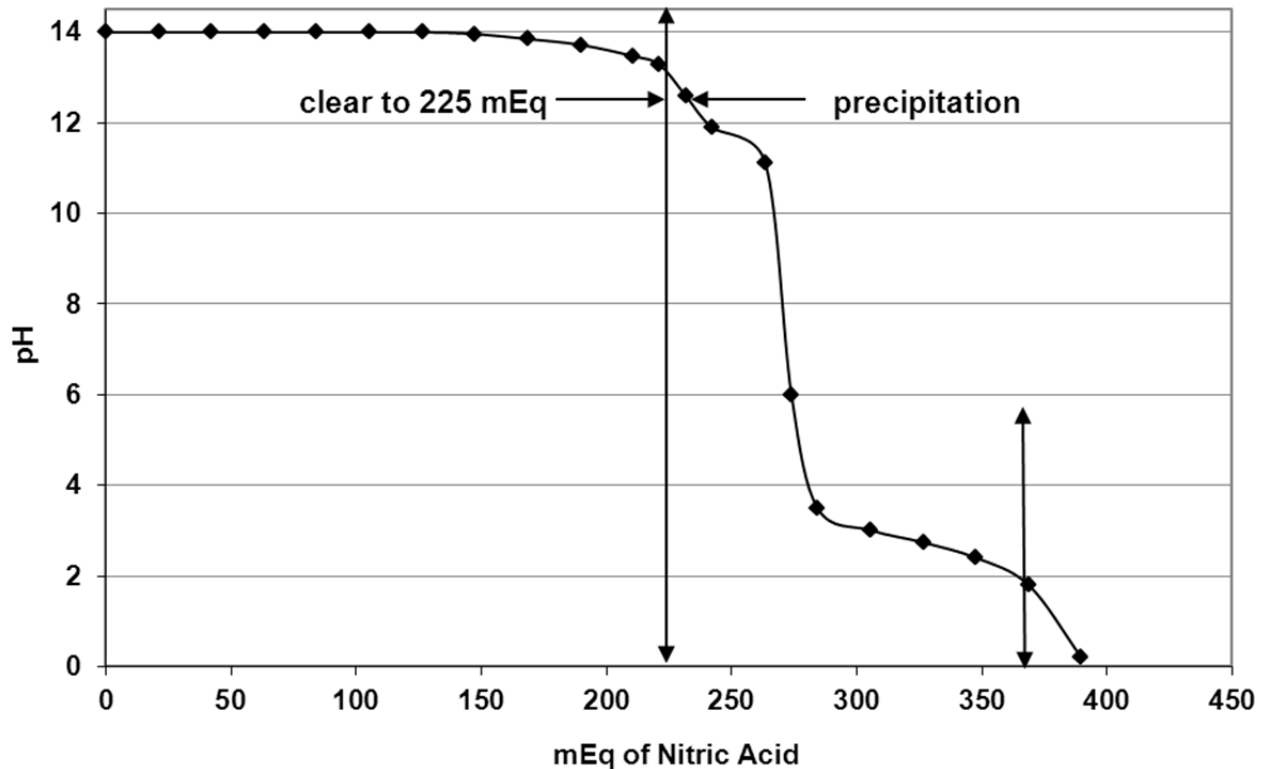


Figure 3.5. Results of titration of 50 mL of the high aluminate simulant precursor with 10 wt % nitric acid. The vertical lines identify the 225 mEq of free hydroxide and the total 375 mEq of hydroxide (includes 150 mEq of bound hydroxide) in 50 mL of this simulant.

The results of the titrations for both precursor simulants demonstrate that precipitation occurs immediately after all of the free hydroxide is neutralized. Additional acid added after this point results in the neutralization of the hydroxides bound to the aluminate, $\text{Al}(\text{OH})_4^-$. The precipitation which accompanies this neutralization of the bound hydroxides is a result of $\text{Al}(\text{OH})_3$ formation. In order to provide a safety factor to prevent this precipitation, it is necessary to reduce the amount of acid added to the system (equivalent to the amount of free hydroxide in solution). A value of 1.0 M free hydroxide ion was selected as a value for the simulants after sodium recovery which provides sufficient safety from precipitation. This corresponds to 150 mEq of acid added to the low aluminate precursor simulant and 175 mEq of acid added to the high aluminate precursor simulant.

In terms of sodium hydroxide recovery using the Ceramatec process, these final states of the two simulants correspond to sodium hydroxide recovery of 56 % for the low aluminate simulant and 44 % for the high aluminate simulant. For comparison, the maximum recovery of sodium hydroxide prior to alumina formation is 75 % for the low aluminate simulant and 57 % for the high aluminate simulant. In this discussion, the sodium hydroxide recovery is based on the initial sodium concentration in the waste stream after aluminum dissolution and the final concentration of sodium after sodium recovery. That is, the percent efficiency, η , for sodium hydroxide recovery, is given by Equation 3.4.

(3.4)

The compositions of the low and high aluminate simulants, reflective of the compositions of the LAW waste streams after both aluminum dissolution and sodium hydroxide recovery with inclusion of a safety

margin to prevent alumina formation are provided in Table 3.2. The densities and wt % solids for the two simulants are also provided in Table 3.2. These simulants did not show any precipitation even after storage at 5 °C.

Table 3.2. Composition, Density and wt % Solids of the Low and High Aluminate Simulants.

Compound	Simulants	
	Low Aluminate (M)	High Aluminate (M)
NaOH	2.000	4.000
NaNO ₃	0.147	0.160
NaNO ₂	0.054	0.050
Na ₂ CO ₃	0.055	0.055
Na ₂ C ₂ O ₄	0.001	0.001
Na ₂ SO ₄	0.001	0.018
Al(NO ₃) ₃	0.250	0.750
Na ₃ (PO ₄)	0.002	0.006
Total Na Molarity	2.32	4.38
Density (g/mL)	1.113	1.224
Wt % Solids	13.77	27.33

3.2.2 Areva Simulant

A second method of sodium recovery, developed by AREVA, precipitates the aluminate in the supernate waste stream as a lithium hydrotalcite (LHT), $\text{Li}_2\text{CO}_3 \cdot 4\text{Al}(\text{OH})_3 \cdot 3\text{H}_2\text{O}$, by addition of lithium hydroxide. The LHT crystalline powder is then filtered and washed. The filtrate (containing the sodium hydroxide and other salts) and spent washes are combined, concentrated and then recycled for aluminum leaching of HLW. The LHT powder is an aluminum rich crystalline material that is part of the layered double hydroxide family of materials. These crystals consist of positively charged aluminate layers separated by layers containing water and anions (carbonate, nitrate, hydroxide etc). The washed LHT is the LAW stream that will be immobilized. There is also the possibility to use LHT, at least in part, as glass formers in WTP.¹⁴

The number of washes of the LHT will depend on operational and regulatory limits, but it could be as high as five. The resultant LHT powder will therefore have relatively small amounts of salts present in the interstitial water. Consequently, the approach taken for this task was to generate the carbonate form of LHT without addition of any of the other common anions (exclusive of OH⁻). To accomplish this, a solution was made to which a 4.6 M LiOH solution was introduced (Table 3.3).¹⁴

Table 3.3. Solutions Used for Generating Lithium Hydrotalcite

Compound	LHT Generation	
	Initial Solution (M)	Added Solution (M)
NaOH	4.50	0.00
NaNO ₃	0.00	0.00
NaNO ₂	0.00	0.00
Na ₂ CO ₃	0.30	0.00
Na ₂ C ₂ O ₄	0.00	0.00
Na ₂ SO ₄	0.00	0.00
Al(NO ₃) ₃	0.80	0.00
Na ₃ (PO ₄)	0.00	0.00
LiOH	0.00	4.60

In this process, the initial solution (1000 g) was heated to 90 °C and then LiOH solution (70 mL) was added at a constant rate over a period of ~ 1 hour. A white precipitate was evident and the slurry was maintained at 90 °C for 3 additional hours. After cooling, the slurry was filtered using a Buchner funnel and the product was collected on a cellulose filter (1452-110, #52) with a particle size cutoff of ~ 7 microns. For this initial test, the product was washed only once, transferred to a drying pan and placed in a 60 °C oven for drying overnight. The powdered product is shown in Figure 3.6. The yield was 46 g of LHT, 65 % of the potential product based on Al and Li concentrations.^{14,19}

**Figure 3.6. Lithium Hydrotalcite product after drying overnight at 60 °C**

A small sample of LHT was dissolved in acid at elevated temperatures for determination of the lithium and aluminum concentrations by Inductively Coupled Plasma (ICP) spectroscopy. The molar ratio of Li/Al determined by ICP was 0.54, which can be compared to the expected value of 0.50. An X-Ray Diffraction (XRD) measurement revealed a pattern consistent with LHT (Figure 3.7).

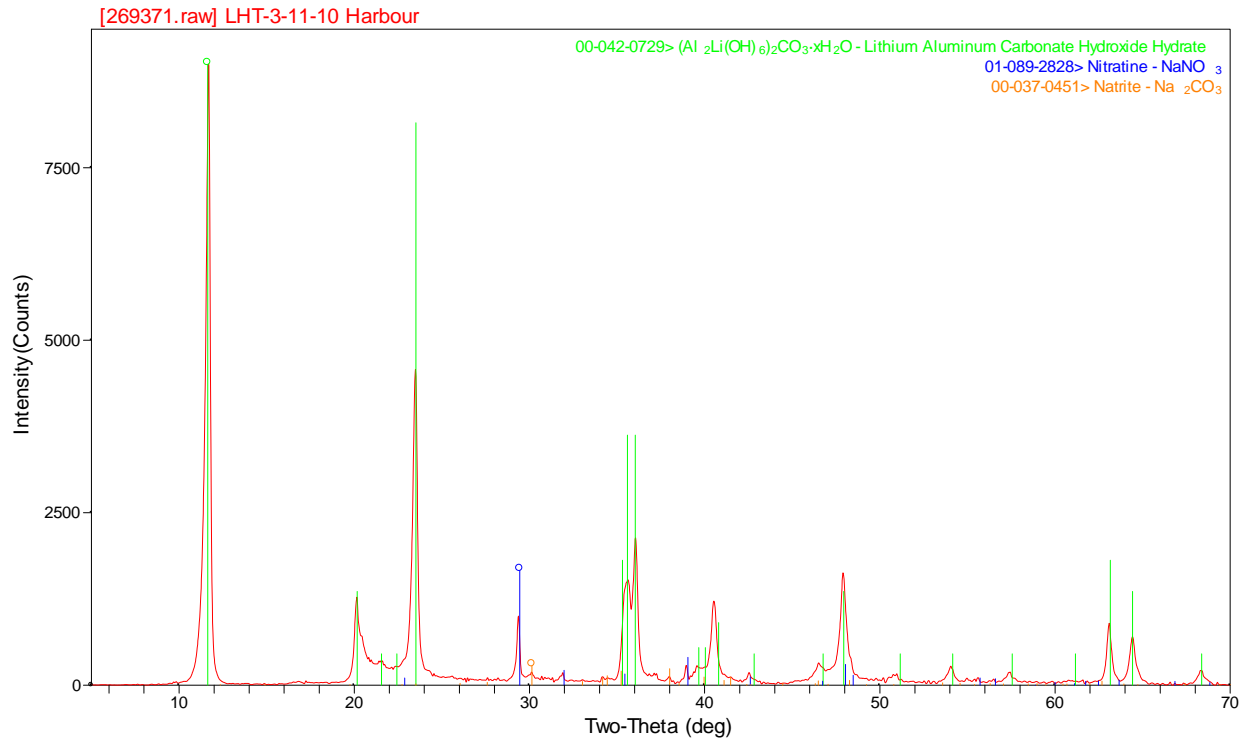


Figure 3.7. XRD pattern for LHT product.

4.0 Immobilization Waste Forms

Methods of immobilization that were considered for the two waste streams include low temperature processes (Saltstone/Cast stone and geopolymers), intermediate temperature processes (steam reforming and phosphate glasses) and high temperature processes (borosilicate glass). These immobilization methods and the waste forms they produce will be evaluated for (1) compliance with the Performance Assessment (PA) requirements for disposal at the IDF, (2) waste form volume (waste loading), (3) compatibility with the tank farms and systems, and (4) feasibility of implementation.³

4.1 Iron phosphate Glass Waste Forms

Immobilization of LAW and HLW waste streams by incorporation into iron phosphate glass waste forms has been considered in general within the DOE Complex and in particular for Hanford.²¹ For this task, an iron phosphate waste form was selected as one of the intermediate temperature waste forms for the LAW streams resulting after CSL and sodium recovery at Hanford.

4.1.1 Formulation

The iron phosphate glass formulations were developed by the MO-SCI Corporation. A number of glasses were fabricated and subsequently evaluated using the ASTM C1285 Product Consistency Test (PCT)²² for both the quenched and canister-center-line cooled (CCC) glasses.[†] Candidate glass waste forms for the high aluminate (HAL) and low aluminate (LAL) were selected based on the sodium normalized release

[†] As there was no previous basis for the cooling curve profile, the WTP LAW ccc profile was adapted from its original form (WSRC-TR-2003-00536). Instead of starting at 1114°C, the profile was started at 1000°C to account for the lower melting temperature of the phosphate glasses.

rates from the PCT. Compositions of these glasses are provided in Table 4.1. Note that Al_2O_3 , Na_2O , P_2O_5 and SO_3 are solely waste components and the remaining oxides are additives. Although the initial formulations of HAL and LAL were quite different, the resulting candidate compositions are coincidentally very similar for both wastes.

Table 4.1. Target and Measured Glass Compositions for the HAL and LAL Iron Phosphate Glasses (wt%).

Oxide	MS-HAL-5		MS-LAL-7	
	Target Composition	Measured Composition	Target Composition	Measured Composition
Al_2O_3	13.60	13.58	13.60	13.47
Na_2O	20.30	19.85	20.34	19.64
P_2O_5	40.04	40.19	40.04	39.62
SO_3	0.21	0.00	0.02	0.00
B_2O_3	2.00	2.05	2.00	5.04
CaO	1.50	1.48	1.50	1.42
Fe_2O_3	10.99	10.90	11.14	11.01
La_2O_3	1.00	0.94	1.00	0.93
SiO_2	5.00	5.18	5.00	5.05
ZnO	4.36	4.59	4.36	4.58
ZrO_2	1.00	0.91	1.00	0.91

4.1.2 PCT

The normalized leachate concentrations²² (g/L) for Na, Si, and Al for the selected glasses are provided in Table 4.2. The ccc glasses exhibit higher release rates than the quenched glasses, but still meet the acceptance criterion of less than 4 g/L. A value of 4 g/L is equivalent to the specification in the WTP contract, which is expressed in terms of surface area (2 g/m^2).²¹

Table 4.2. Normalized Concentrations for the HAL and LAL Phosphate Glasses

Sample ID		MS-HAL-5	MS-HAL-5ccc	MS-LAL-7	MS-LAL-7ccc	
Normalized Release Rate (g/L)	Target	Al	0.63	1.24	0.62	1.24
	Measured		0.63	1.24	0.62	1.25
	Target	Na	1.67	1.83	1.61	1.74
	Measured		1.70	1.87	1.67	1.80
	Target	P	0.89	0.82	0.88	0.81
	Measured		0.88	0.82	0.89	0.82
	Target	Si	0.70	1.19	0.68	1.23
	Measured		0.68	1.14	0.67	1.22

¹ Release rates are normalized to both the target and measured compositions.

4.1.3 Vapor Hydration Test (VHT)

The corrosion rates of MS-HAL-5ccc and MS-LAL-7ccc were calculated to be 715 g/m² and 635 g/m², respectively.²³ Corrosion rates for the quenched versions of these glasses were not performed. Neither of these glasses are acceptable in terms of the 50 g/m² limit.²¹ Photos of the tested materials are shown in Figure 4.1.

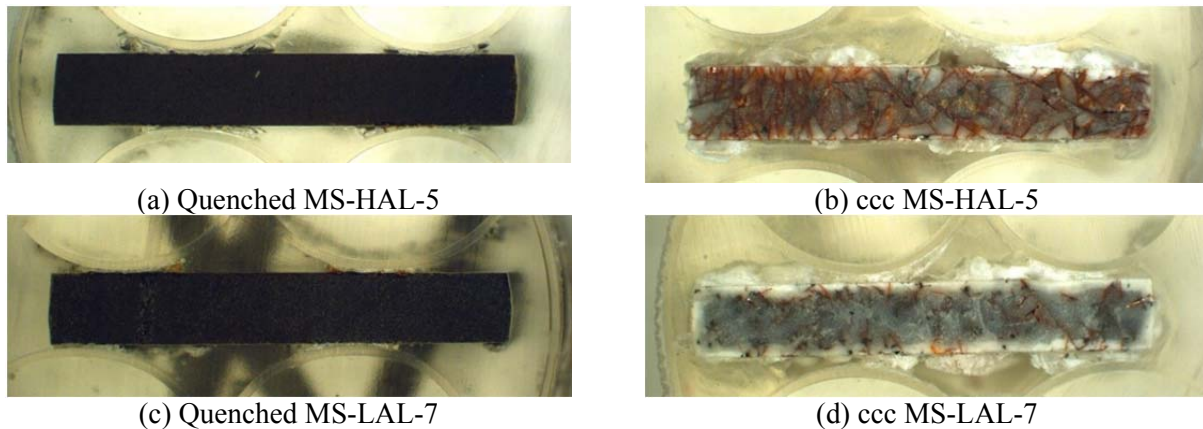


Figure 4.1. Images of the VHT samples for (a) quenched MS-HAL-5, (b) ccc MS-HAL-5, (c) quenched MS-LAL-7 and (d) ccc MS-LAL-7.

4.1.4 XRD

X-ray Diffraction (XRD) data for these glasses are provided in Figure 4.2 through Figure 4.5. Both of the quenched glasses are amorphous; however, the ccc versions of these glasses do contain various crystalline phases.[‡] The best matches for the ccc sample of MS-LAL-7 include sodium iron phosphate and a phase

[‡] Difficulties were encountered during analysis of the XRD spectra. Many of the crystals listed are best matches; however, they are not exact matches to the peaks of the LAL and HAL samples. In some cases, not all of the peaks could be identified.

similar to sodium praseodymium phosphate[§], while MS-HAL-5ccc may contain sodium iron phosphate, hematite and a phase similar to sodium lanthanum phosphate.

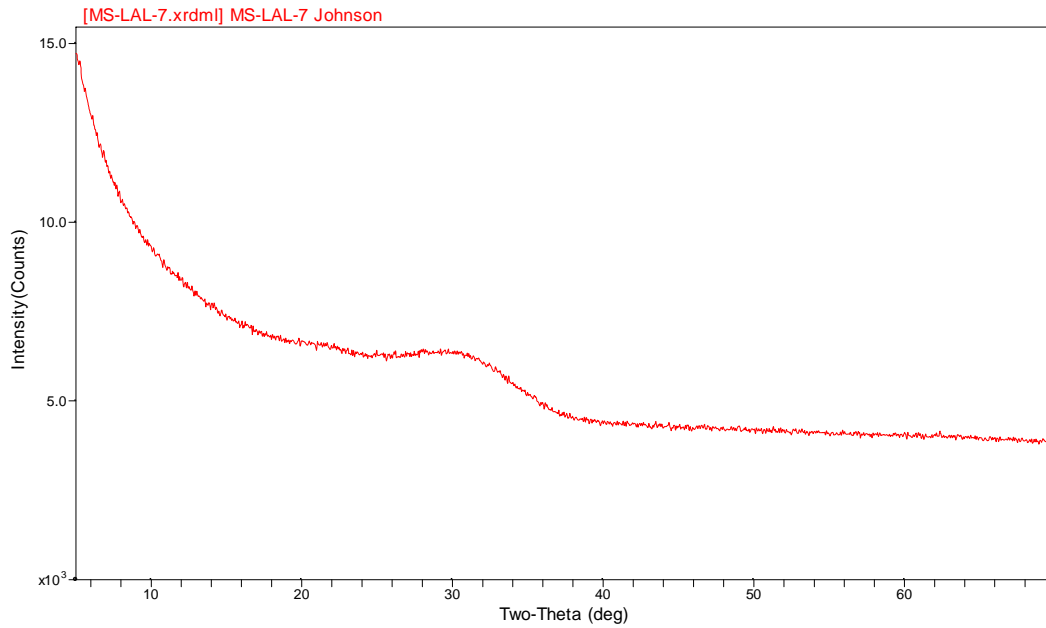


Figure 4.2. XRD data for quenched MS-LAL-7 glass typical of an amorphous glass.

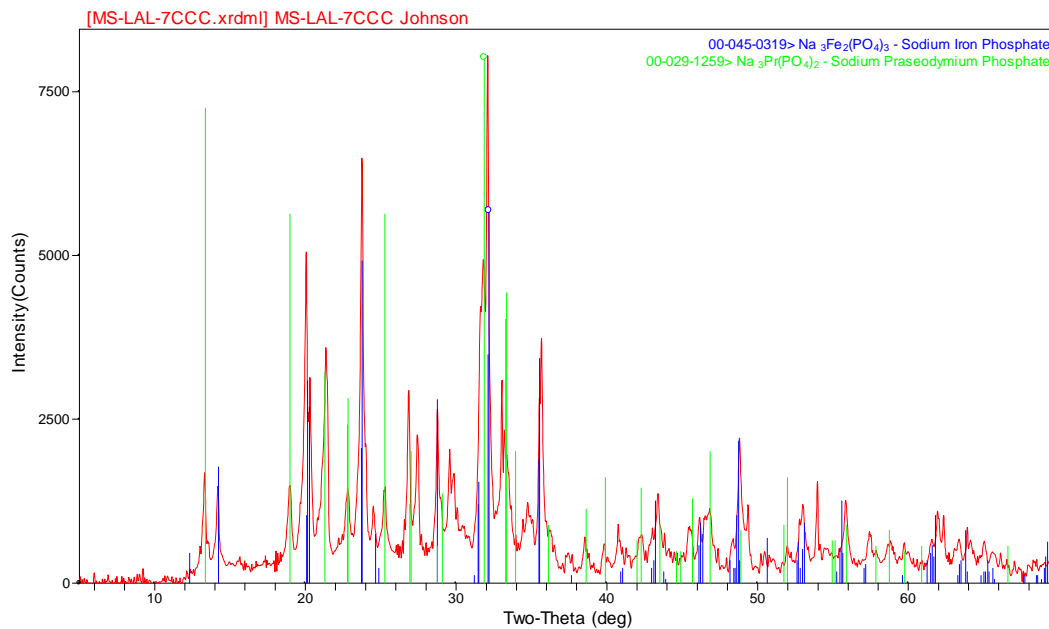


Figure 4.3. XRD data for ccc MS-LAL-7 glass showing at least two crystallites within the glass matrix.

[§] Praseodymium is not present in these glasses, but it is likely that there is some type of substitution occurring for a similar element.

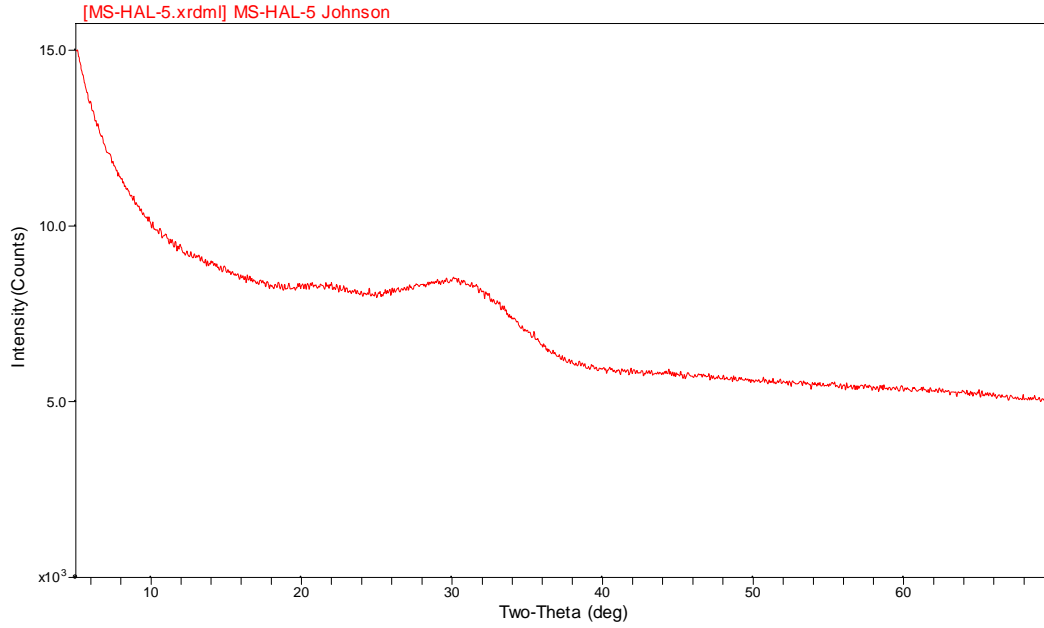


Figure 4.4. XRD data for quenched MS-HAL-5 glass typical of an amorphous glass.

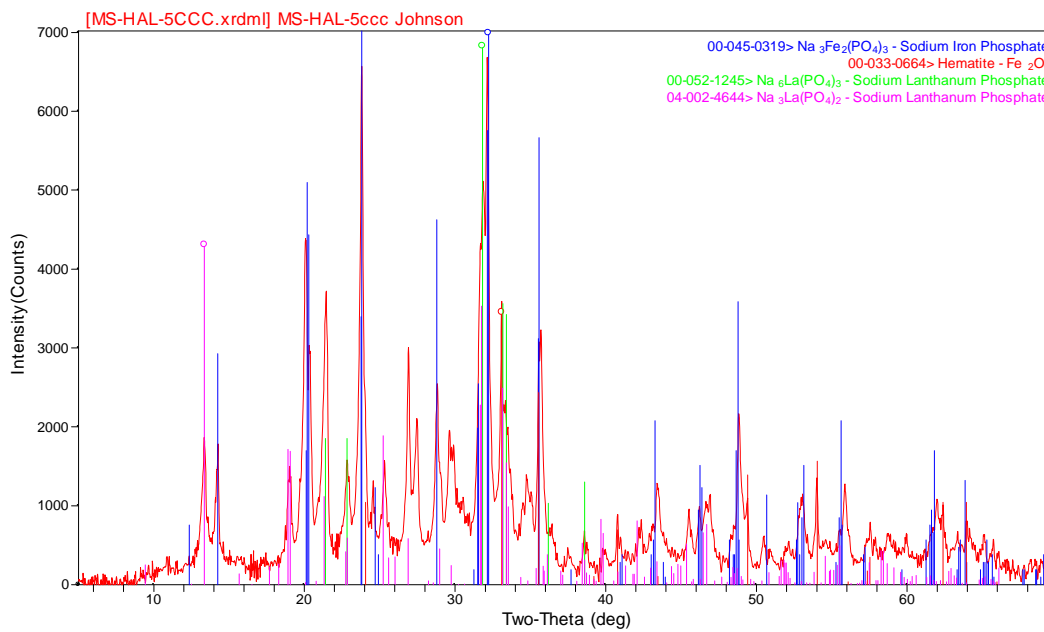


Figure 4.5. XRD data for ccc MS-HAL-5 glass showing approximately four crystalline phases within the glass matrix.

4.1.5 Volume and Mass Factors

The volume and mass of the waste form produced for each liter of LAW waste stream is provided in Table 4.3. The volume of waste is reduced by a factor of 0.12. The total mass is reduced by a factor of 0.32. All of the sodium was introduced in the waste streams such that the waste loading of Na₂O on a mass basis was 20.3 %.

These initial formulations did not include Re and I. Additional experimental work will be required to include Re and I into the glass formulations with these elements to simulate I-129 and Tc-99 in the waste stream. The glasses prepared with the surrogates will then be subjected to the same analysis and leach testing performed in this study.

Table 4.3. Volume and Mass of Waste Form Produced per Liter of LAW with Phosphate Glass

Volume of Waste	Volume of Glass	Volume Factor	%Na ₂ O
(L)			
1.0	0.12	0.12	
Mass of Waste	Mass of Glass	Mass Factor	Mass Basis
(g)			
~1100	354	0.32	20.3

4.2 Borosilicate Glass Waste Forms

Another immobilization option is to vitrify Hanford LAW and HLW waste streams as borosilicate glass. The Hanford LAL composition is different from the compositions of the waste streams identified for this task and are therefore outside the envelope of current formulations for LAL. This also applies to the borosilicate glass formulations developed as part of the bulk vitrification option. Therefore, new formulations were developed for these waste streams that provide the baseline case through which to compare the results on the other waste forms tested in this program.

4.2.1 Formulation

In previous work, glasses were fabricated and subsequently tested and evaluated by PCT leaching for both the quenched and CCC glasses.** Glass compositions for the HAL and LAL wastes were selected based normalized release rates determined from the PCT. Target and measured compositions are provided in Table 4.4.

** As stated in the previous section, there was no previous basis for the cooling curve profile, so the WTP LAW ccc profile was adapted from its original form (WSRC-TR-2003-00536). Instead of starting at 1114 °C, the profile was started at 1200 °C to account for the higher melting temperature of the borosilicate glasses. The samples were cooled at a rate of 10°C/min to 1114 °C, at which point the original profile was followed.

Table 4.4. Target and Measured Glass Compositions for the HAL and LAL Borosilicate Glasses (wt%)

Oxide	FCJHAL1		FCJLAL3	
	Target Composition	Measured Composition	Target Composition	Measured Composition
Al ₂ O ₃	6.53	6.45	6.60	6.51
Na ₂ O	23.16	22.07	25.33	24.23
P ₂ O ₅	0.08	0.00	0.05	0.00
SO ₃	0.24	0.25	0.02	0.00
B ₂ O ₃	9.00	9.19	8.00	8.45
CaO	2.00	2.00	2.00	2.02
Fe ₂ O ₃	6.00	5.53	5.50	5.13
MgO	1.60	1.42	1.60	1.43
SiO ₂	45.00	43.44	44.50	43.34
TiO ₂	1.01	0.95	1.01	0.96
ZnO	2.00	1.80	2.00	1.85
ZrO ₂	3.38	3.06	3.39	3.15

4.2.2 PCT

The normalized leachate concentrations in g/L for Na, Si, and Al for the selected glasses are provided in Table 4.5. The ccc glasses show lower release rates for B and Na than the quenched glasses and all glasses meet the acceptance criterion of < 4 g/L. A value of < 4 g/L is equivalent to the specification in the Contract which is expressed in terms of surface area (< 2 g/m²).²¹

Table 4.5. Normalized Concentrations for the HAL and LAL Borosilicate Glasses

Sample ID		FCJHAL-1	FCJHAL-1ccc	FCJLAL-3	FCJLAL-3ccc	
Normalized Release Rate (g/L)	Target	B	0.94	0.78	1.07	0.95
	Measured		0.92	0.77	1.01	0.89
	Target	Na	0.95	0.87	1.19	1.08
	Measured		1.00	0.92	1.24	1.13
	Target	Si	0.39	0.37	0.48	0.45
	Measured		0.40	0.39	0.49	0.47

¹ Release rates are normalized to both the target and measured compositions.

4.2.3 Vapor Hydration Tests

VHT²³ results are presented in Table 4.6. Because the samples cracked, there is no method for determining a corrosion rate. Only the ccc sample of FCJHAL-1 is acceptable with respect to the limit of 50 g/m².²¹ Photos of the tested materials are shown in Figure 4.6.

Table 4.6. Summary of VHT Results for HAL and LAL Borosilicate Glasses

Sample ID	Corrosion	Notes
FCJHAL-1	65 g/m ²	NA
FCJHAL-1ccc	27 g/m ²	
FCJLAL-3	~50%	Sample expanded. Some cracks go all the way through sample.
FCJLAL-3ccc	~50%	Sample expanded. Some cracks go all the way through sample.

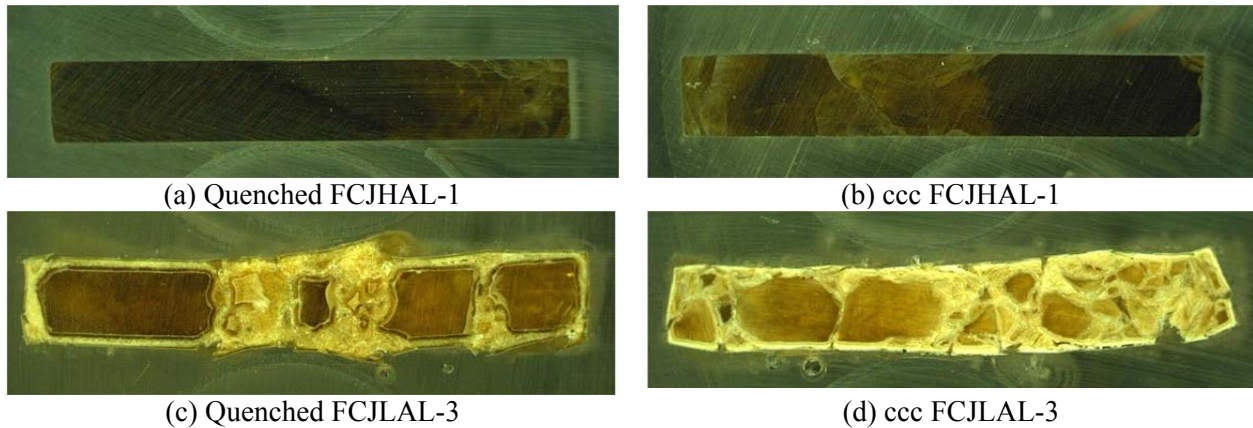
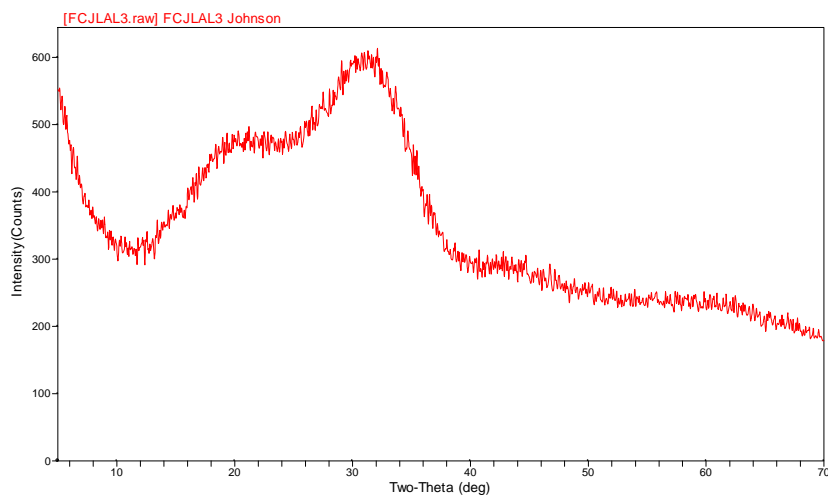


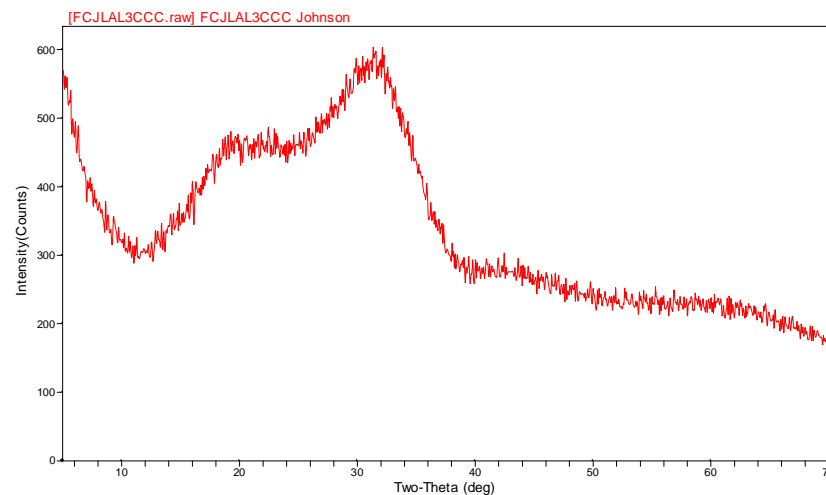
Figure 4.6. Images of the VHT samples for (a) quenched FCJHAL-1, (b) ccc FCJHAL-1, (c) quenched FCJLAL-3 and (d) ccc FCJLAL-3.

4.2.4 X-ray Diffraction

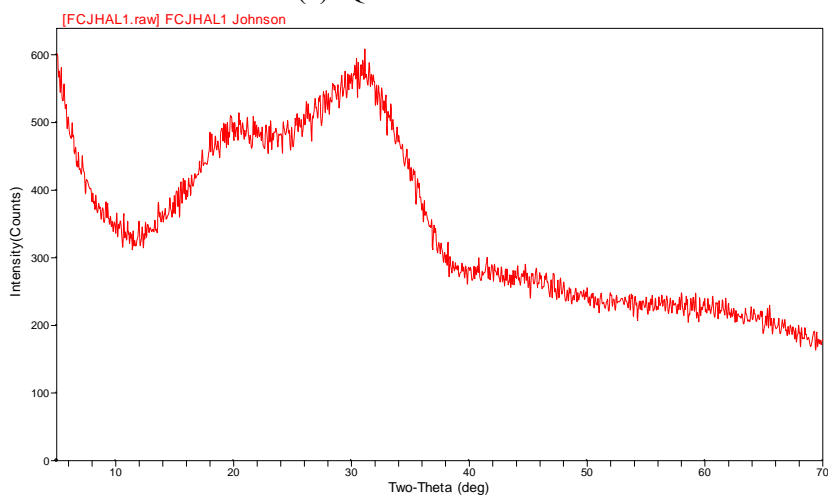
XRD data for these glasses are provided in Figure 4.7. Both the quenched and ccc versions of the HAL and LAL glasses are amorphous.



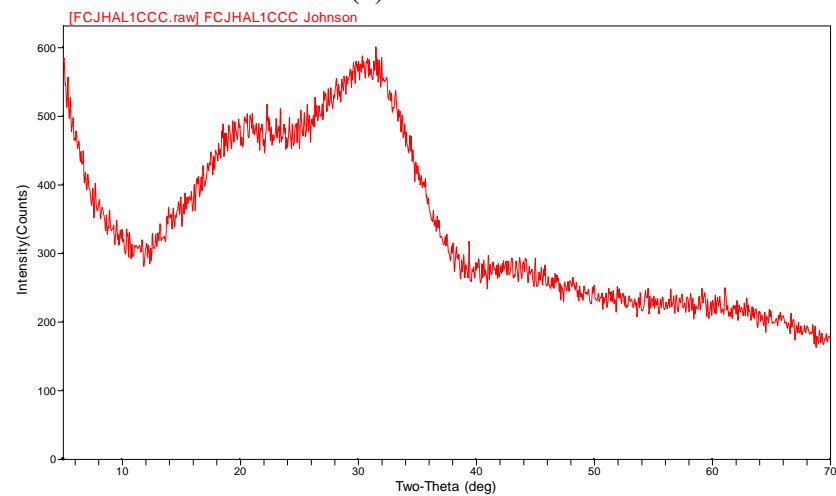
(a) Quenched FCJLAL-3



(b) FCJLAL-3ccc



(c) Quenched FCJHAL-1



(d) FCJHAL-1ccc

Figure 4.7. XRD spectra of the (a) quenched FCJLAL-3 glass, (b) FCJLAL-3ccc glass, (c) quenched FCJHAL-1 glass and (d) FCJHAL-1ccc.

4.2.5 Volume and Mass Factors

The volume and mass of the waste form produced for each liter of LAW is provided in Table 4.7. The volume of waste is reduced by a factor of 0.10. The total mass is reduced by a factor of 0.26. All of the sodium was introduced in the waste streams such that the waste loading of Na₂O on a mass basis was 25.4 %.

Table 4.7. Volume and Mass of Waste Form Produced per Liter of LAW with Borosilicate Glass

Volume of Waste	Volume of Glass	Volume Factor	%Na ₂ O
(L)			
1.0	0.10	0.10	
Mass of Waste	Mass of Glass	Mass Factor	Mass Basis
(g)			
~1100	282	0.26	25.4

4.2.6 Doped Glasses

Glasses were also batched for FCJLAL-3 and FCJHAL-1 compositions with 0.57 wt % I and 0.2 wt % Re₂O₇ added to simulate I-129 and Tc-99 in the waste stream, which are denoted as FCJLAL-3D and FCJHAL1-D. These two radionuclides are important to the Performance Assessment (PA) for the IDF at Hanford. A comparison of the target and measured compositions are provided in Table 4.8. A batching error occurred for FCJHAL-1D and no ZrO₂ was added to the glass. In general, the rest of the measured main components of the glass are consistent with the target values. The dopant concentrations are low; however, the analytical methods used for evaluating those constituents are being evaluated. It is possible that the dopants were vaporized during melting or during preparation of the samples for analysis.

The normalized PCT release rates are provided in Table 4.9. All of the values are acceptable with respect to the 4 g/L limit specified in the WTP contract. Leaching results for I and Re for the LAL and HAL glasses are provided in Table 4.10.

VHT results are presented in Table 4.11. There is no method for determining a corrosion rate since the samples were cracked. Thus, none of the samples exhibited corrosion rates that were less than the limit of 50 g/m² per day. Photos of the tested materials are shown in Figure 4.8. The anomalous behavior exhibited by the FCJHAL1D samples can be attributed to the lack of ZrO₂ in the batched material.^{††}

^{††} Increased concentrations of ZrO₂ have been shown to significantly improve the VHT corrosion rate.

Table 4.8. Target and Measured Compositions for the Doped HAL and LAL Borosilicate Glasses (wt%)

Oxide	FCJHAL-1D		FCJLAL-3D	
	Target Composition	Measured Composition	Target Composition	Measured Composition
Al ₂ O ₃	6.53	6.76	6.60	6.70
Na ₂ O	23.16	23.15	25.33	25.31
P ₂ O ₅	0.08	0.00	0.05	0.00
SO ₃	0.24	0.26	0.02	0.00
B ₂ O ₃	8.90	9.26	7.91	7.79
CaO	1.98	2.12	1.98	2.18
Fe ₂ O ₃	5.93	6.03	5.44	5.23
MgO	1.58	1.52	1.58	1.46
SiO ₂	44.50	46.12	44.00	45.05
TiO ₂	1.01	0.98	1.00	0.95
ZnO	1.98	1.96	1.98	1.95
ZrO ₂	3.34	0.00	3.35	3.10
Dopants				
Re ₂ O ₇	0.20	0.14	0.20	0.14
I	0.57	0.18	0.57	0.24

Table 4.9. Normalized Concentrations for the Doped HAL and LAL Borosilicate Glasses

Sample ID		FCJHAL-1D	FCJHAL-1Dccc	FCJLAL-3D	FCJLAL-3Dccc	
Normalized Release Rate (g/L)	Target	B	1.81	1.31	1.29	1.21
	Measured		1.74	1.26	1.31	1.23
	Target	Na	1.59	1.25	1.44	1.33
	Measured		1.59	1.25	1.44	1.33
	Target	Si	0.66	0.58	0.51	0.53
	Measured		0.64	0.56	0.50	0.52

Table 4.10. Re and I Leachate Results

Sample ID	Re	I
	(ppm)	
FCJHAL1D	1.19	0.65
FCJHAL1Dccc	0.68	0.17
FCJLAL3D	1.03	2.08
FCJLAL3Dccc	0.88	0.99

Table 4.11. Summary of Corrosion Results for the Doped HAL and LAL Borosilicate Glasses

Sample ID	Corrosion	Notes
FCJHAL-1D	100%	Center of sample is void.
FCJHAL-1Dccc	100%	Center of sample is void.
FCJLAL-3D	~90%	Sample expanded. Some cracks go all the way through sample.
FCJLAL-3Dccc	~50%	Sample expanded. Some cracks go all the way through sample.

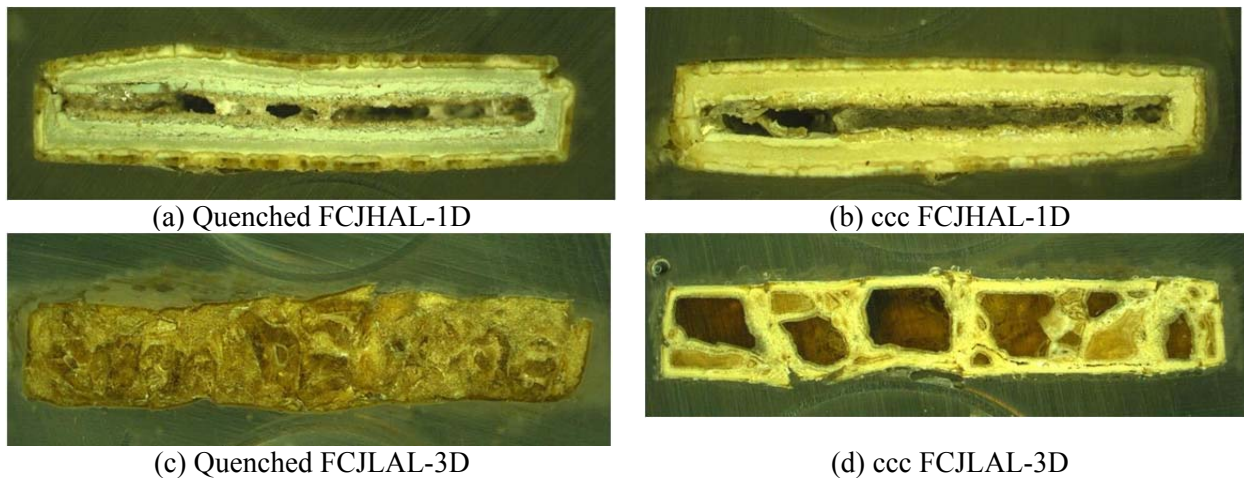


Figure 4.8. Images of the VHT samples for (a) quenched FCJHAL-1D, (b) ccc FCJHAL-1D, (c) quenched FCJLAL-3D and (d) ccc FCJLAL-3D.

4.3 Steam Reformed Waste Form

One immobilization option for the Hanford LAW waste stream after sodium recovery is Fluidized Bed Steam Reforming (FBSR). This method is already under evaluation for Hanford LAW through EM-31. Due to process scale, the steam reformed waste form was prepared using the SRNL Bench Scale Steam Reformer (BSR).

FBSR is being considered as an alternative technology for the immobilization of a wide variety of aqueous high sodium containing radioactive wastes at various DOE facilities.²⁴ The addition of clay, charcoal, and a catalyst as co-reactants converts aqueous LAW to a granular or “mineralized” waste form while converting organic components to CO₂ and steam through pyrolysis, and nitrate/nitrite components to N₂.²⁴ The waste form produced is a multiphase mineral assemblage of Na-Al-Si feldspathoid minerals with cage-like structures that immobilize radionuclides.²⁴ If carbon is the only additive to the waste stream, then a solid carbonate product will be formed. This product is water soluble making it easy for further processing such as to a slurry fed glass melter. If sodium-aluminosilicates are added as well, then a final waste form can be produced for storage in drums. This form can also be captured in a cementitious monolith.²⁵

4.3.1 Formulation

Formulations for the steam reformed product utilized both the low and high aluminate waste streams. The projected BSR waste form composition²⁶ for each waste stream is shown on the Na₂O-SiO₂-Al₂O₃ ternary diagram (Figure 4.9). The projected formulation is the AN-107 FBSR product shown by the blue square on the ternary diagram. Optikast and Sagger mixed clays were used based on the amount and composition of the simulat used in the formulation according to the algorithm²⁶ used to obtain the desired mineral product. Coal is added as a reductant to destroy the nitrates present in the salt solution waste stream. In addition, the coal serves as the energy source for the exothermic reaction.

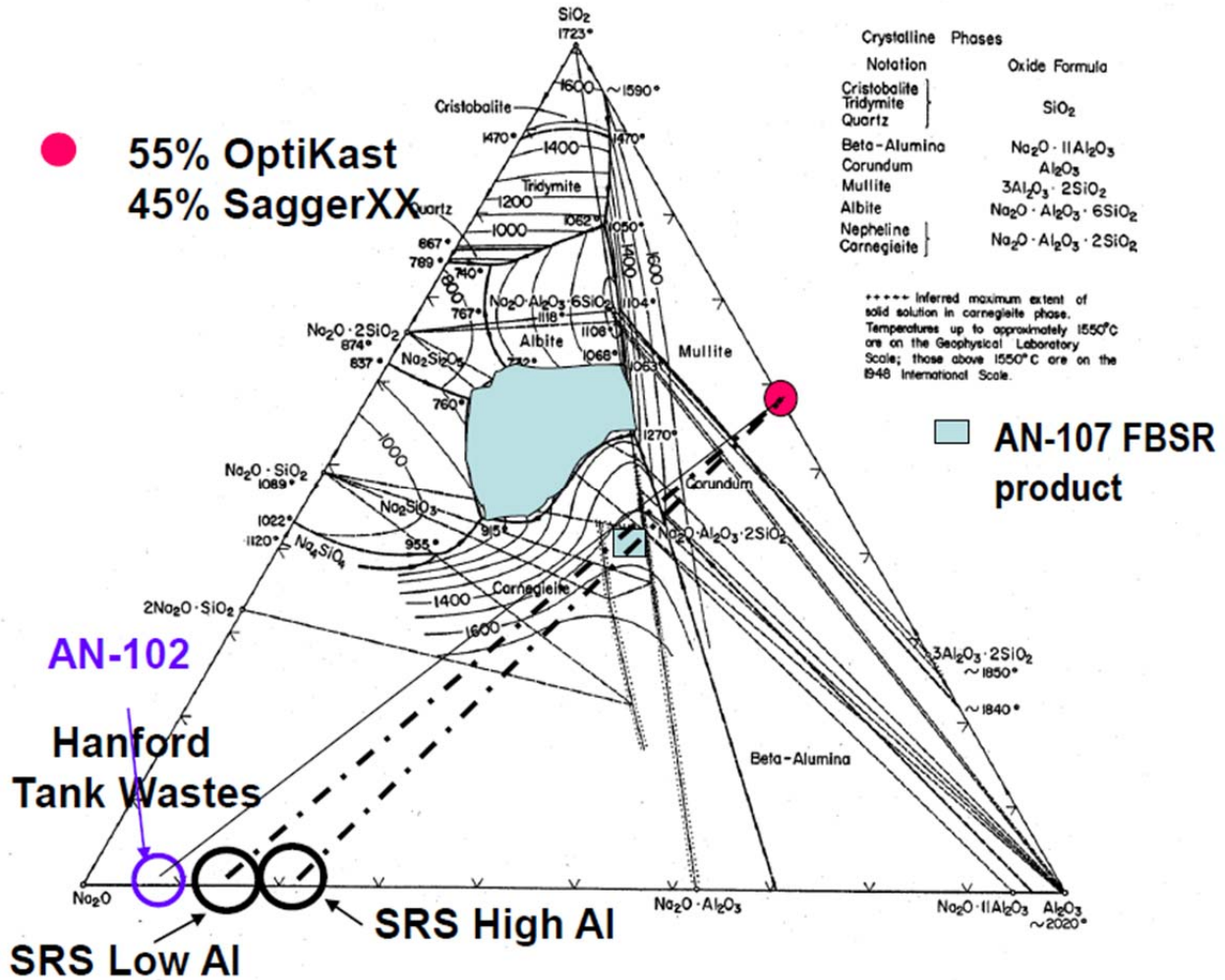


Figure 4.9. Na₂O-SiO₂-Al₂O₃ ternary diagram showing the projected steam reformed waste form composition (blue square) for high and low aluminate waste streams.

4.3.2 BSR Equipment Setup

The BSR designed at SRNL is a two-stage unit used to produce the same mineralized products and gases as the FBSR (Figure 4.10). Unlike the FBSR, the BSR is not fluidized since it was designed to fit in the shielded cells and there is not enough height in the cells to allow for product disengagement. Steam does flow though the product freely. Only the first stage or De-nitration Mineralization Reactor (DMR) was used for this study.²⁷

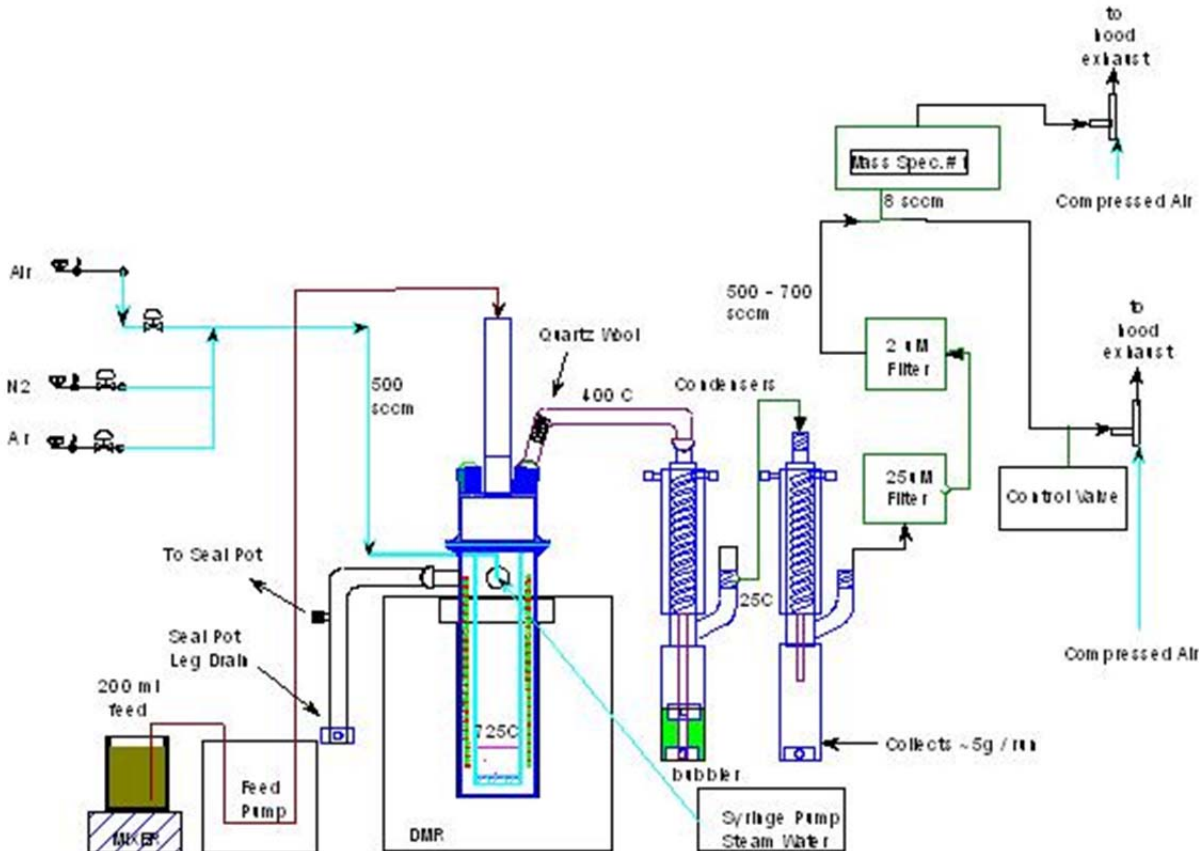


Figure 4.10. Schematic of the Bench-Scale Steam Reformer.

The SRNL BSR DMR inner reaction chamber dimensions are 70 mm ID x 385 mm tall with a porous bottom. The bottom 50 mm (2 inches) is filled with yttria-stabilized zirconia beads Figure 4.11. The zirconia beads were heavy enough not to be suspended by the gases and steam flowing up past them, acted as a base for the product to form on, allowed easy removal of the product from the reaction chamber, allowed easy separation of the product from the beads for analytic purposes, and provided a heat transfer medium for the gases that flow up through them.^{25,27}

The DMR outer chamber dimensions are 120 mm ID x 400 mm tall and provides connections for the outer chamber pressure relief and measurement line, and each of the two 20 foot coils which are housed between the DMR inner reaction chamber and the outer chamber. The outer chamber is sealed by the top flange of the inner chamber, and thus has a pressure relief line going to a seal pot which relieves at about 15 inwc. Water, N₂, Ar, and air enter the DMR via the coils which are between the inner and outer walls of the DMR and are converted to superheated steam and hot gases with heat provided by the furnace that contained the DMR. The steam and gases exit the coils and flow through the bottom of the DMR inner reaction chamber, the zirconia beads, the product, and finally flow out through the top of the DMR to the DMR condenser. The N₂, Ar, and Air total flow rates were held at a constant to improve process control.^{25,27}

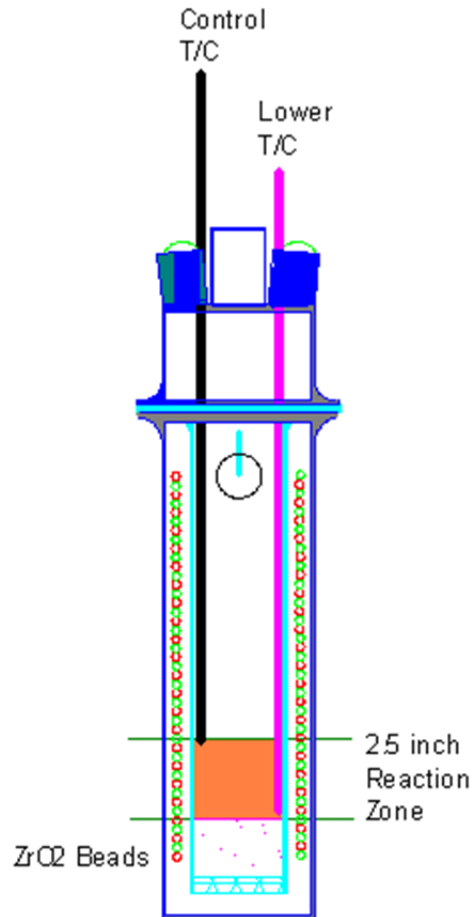


Figure 4.11. DMR chamber showing the 2.5 inch reaction zone.²⁷

During a typical run, the feed slurry was kept agitated with a stir bar mixer while a peristaltic pump fed the slurry through the center feed port in the lid of the DMR. A mineralized product formed in the DMR (Figure 4.11) in the presence of superheated steam, clay, and carbon and the off-gases flow toward the DMR condenser.

4.3.3 BSR Processing Conditions

The processing parameters used in the BSR are scaled from the actual FBSR parameters (Table 4.12). The first two data columns in Table 4.12 show the parameters in different units. The feed rate of ~1 ml/min for the DMR was established based on the equipment's ability to pump the clay/coal/waste slurries and the DMR's ability to convert it to mineral product without the presence of unreacted product. Coal was fed at a rate of 0.20 g/min, which is less than the 0.35 g/min scaled equivalent because the BSR does not use coal to auto-catalytically heat the DMR and excess unreacted coal in the product is undesirable. Total gas flow was limited based on observed solids carry over. The DMR temperatures were the same as in the engineering and pilot scale FBSR. The BSR ran at a slightly negative pressure where the FBSR runs at a slightly positive pressure.²⁷

Table 4.12. Relative Scaling of Process Operating Parameters of the BSR Compared to the FBSR for the Hanford LAW simulants.

Parameter	FBSR	Scaled BSR	Actual BSR
Feed Rate	757 ml/min	1 ml/min	1 ml/min
Coal Rate	265 g/min	0.35 g/min	0.2 g/min
Gas Rate	2885 SLM	3.8 SLM	0.5 SLM
Steam Rate			24 ml/hr
H ₂ Conc.	1 – 2%		1.5% - 3%
O ₂ Conc.			< 2%
DMR Temp.	720 °C		725 °C
Pressure	Positive		-2 inwc

4.3.4 XRD

The XRD plots in Figure 4.12 and Figure 4.13 confirm the predicted mineral phases, nepheline, quartz, and nosean²⁶ are present in the samples. Based on the projected compositions shown in Figure 4.9, the high aluminate content has an additional alumina (corundum) mineral present in the waste form.

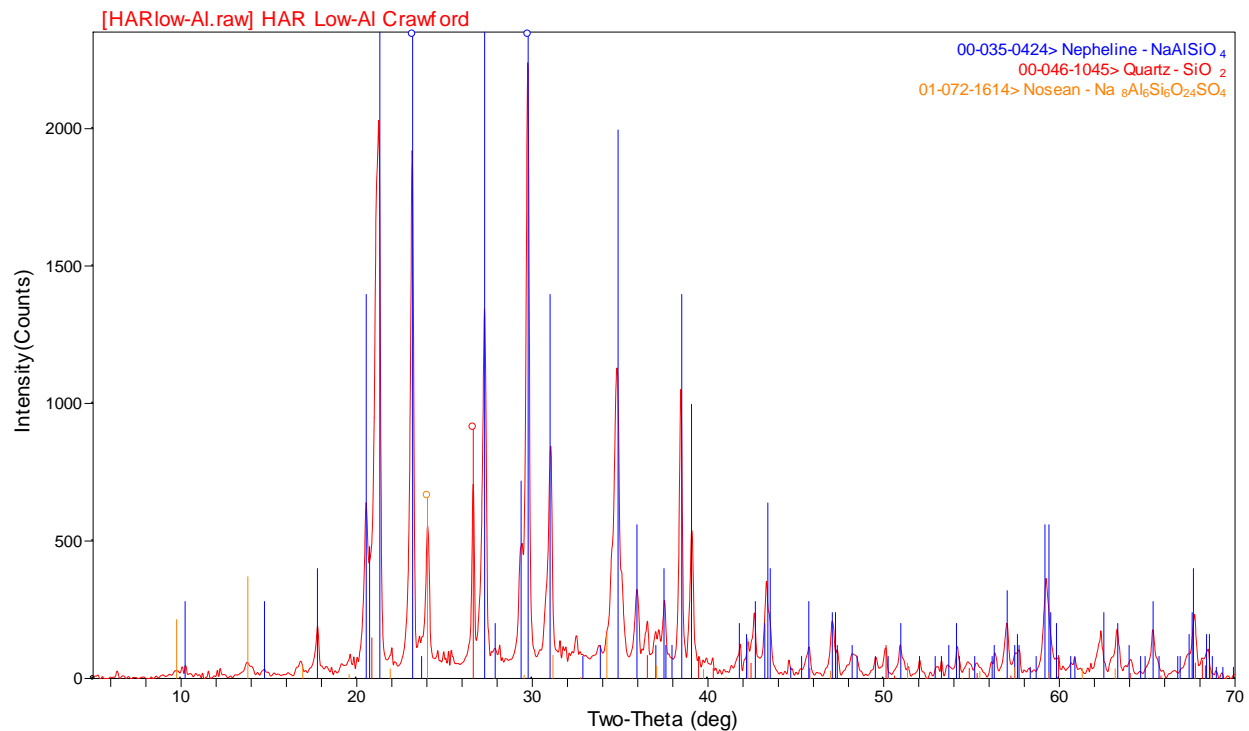


Figure 4.12. XRD plot of BSR product formulated with low aluminate simulant. Phases present are expected based on ternary phase diagram.

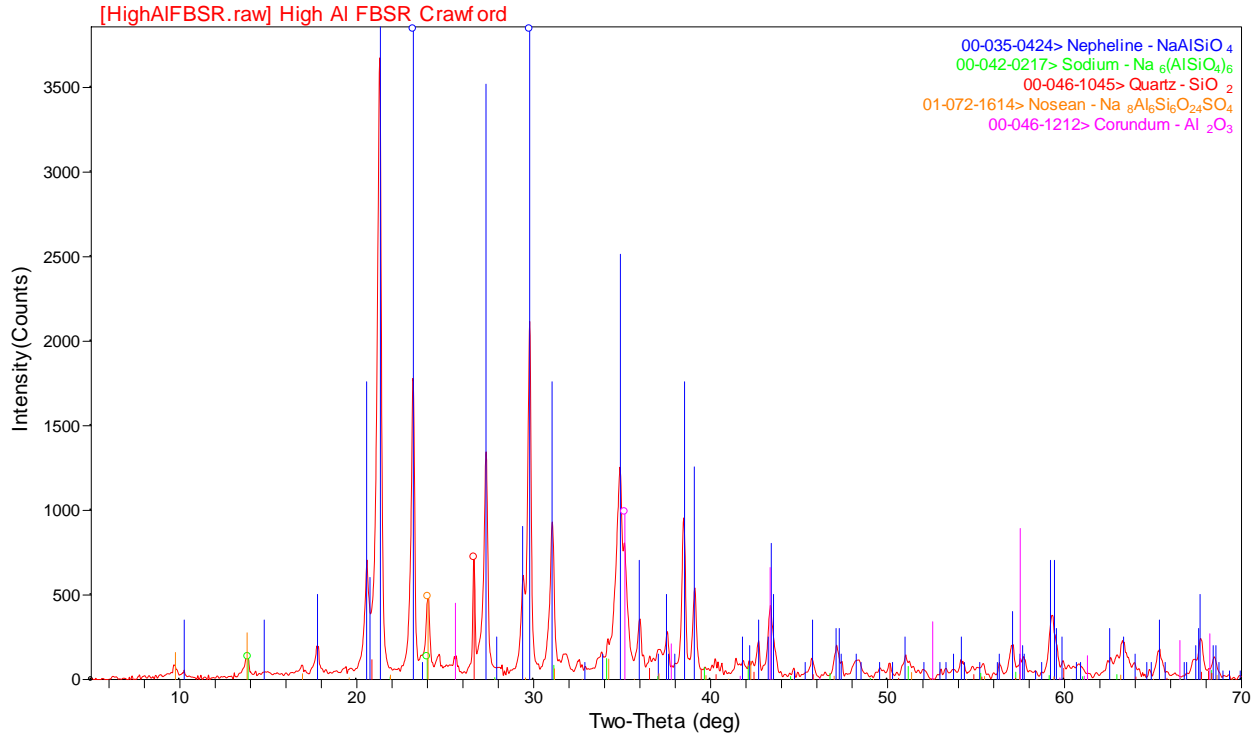


Figure 4.13. XRD plot of BSR product formulated with high aluminate simulant. Phases present are expected based on ternary phase diagram.

4.3.5 Projected Waste Loadings

The projected waste volume and mass factors for the BSR monolith product are listed in Table 4.13. The predicted waste loadings were not confirmed since monoliths of the BSR product were not prepared at the time of this report.

Table 4.13. Projected Waste Loadings for BSR Monolith Product.

By Volume in Monolith Product		
Volume of Waste (L)	Volume of Monolith (L)	Volume Factor
1.0	0.49 – 0.56	0.49 – 0.56
By Mass in Monolith Product		
Mass of 1 L of Waste (g)	Mass of Monolith (g)	Mass Factor
1086 – 1147	917 – 1049	0.84 – 0.92

4.4 Geopolymer Waste Forms

The overall approach for low temperature geopolymeric waste forms consisted of immobilization of the LAW waste streams after aluminum dissolution (stream # 1) and after aluminum dissolution and NaOH recovery (stream # 2). Geopolymers require alkali activation and the LAW stream # 1 already has a sufficient concentration of alkali and can therefore be immobilized directly thereby eliminating the NaOH

recovery step. This alternative removes the need for the additional NaOH recovery process but must be balanced against the use of higher quantities of NaOH. At this stage of the task, only direct geopolymerization of the low aluminate waste stream # 1 has been performed.

Geopolymers are produced through activation of aluminosilicate materials. Typical activating solutions include alkali hydroxide and alkali silicates, where the alkali is typically sodium or potassium. Aluminosilicate sources for geopolymer synthesis typically consist of fly ash, blast furnace slag, or metakaolin. Fly ash, in particular Class F fly ash²⁸, has been the subject of several studies on geopolymers.²⁹⁻³¹ This class of fly ash has a lower calcium content and higher aluminum and silicon content when compared to Class C fly ashes. Aluminosilicate powders that also have high calcium contents may lead to formation of some portland cement reaction products such as calcium silicate hydrate or calcium hydroxide. The combination of both types of reaction product may lead to a weakened material.³² The design of geopolymer mixtures has typically been done using trial-and-error methods to select the proper activating solution, aluminosilicate powder, and curing conditions. Geopolymer mixture proportions have not yet been developed based on thorough knowledge of the constituent materials found in the fly ash, since a definition of- and testing method for- reactive constituents has not yet been developed. A trial and error approach was used in the current task for developing geopolymer mixtures for immobilization of the waste streams 1 and 2.

4.4.1 Cementitious Materials and Simulants

The fly ashes selected spanned a range of calcium contents, with two being classified as Class F fly ash based on ASTM C618²⁸ and the third as Class C. The choice to select fly ashes based on calcium content was made because calcium is often indicated as an important factor in early strength gains when geopolymers are cured at room temperature.³³ The granulated blast furnace slag was obtained from Holcim (directly from the SRS Saltstone Production Facility (SPF)) and tested both as the sole aluminosilicate powder and as a replacement for portions of the fly ash in geopolymer mixtures. Table 4.14 summarizes the chemistry of the raw materials.

Table 4.14. Oxide compositions of aluminosilicate powders based on Inductively Coupled Plasma-Emission Spectroscopy (ICP-ES).

Oxide	Aluminosilicate Source (weight %)			
	Big Brown FA	Belews Creek FA	Boral Class C FA	Holcim BFS
Al ₂ O ₃	18.4	30.5	17.2	7.5
CaO	14.1	1.2	25.3	36.7
Fe ₂ O ₃	8.0	4.6	5.9	0.4
K ₂ O	1.1	2.3	0.6	0.4
MgO	2.2	0.7	5.9	13.0
Na ₂ O	0.6	0.3	2.0	0.3
SO ₄	0.8	0.1	1.7	1.7
SiO ₂	48.3	55.8	35.7	39.2
TiO ₂	1.2	n/a	1.2	0.4
total:	94.9	95.4	96.5	99.5

The caustic activating solutions used for these mixtures were simulant solutions for radioactive salt solutions after caustic leaching of Hanford HLW (waste stream # 1). The compositions are summarized in Table 4.15. The free hydroxide molarity for the low aluminate simulant was 4 M and the free hydroxide molarity for the high aluminate simulant was 4.5 M. The molarity of each constituent in the simulants is shown in Table 4.15. At the time of this report only the low aluminate mixes are discussed.

Table 4.15. Chemical Constituents and Concentrations of Simulants.

Compound	Low Aluminate (moles/L)	High Aluminate (moles/L)
NaOH	5.000	7.500
NaNO ₃	0.147	0.160
NaNO ₂	0.054	0.050
Na ₂ CO ₃	0.055	0.055
Na ₂ C ₂ O ₄	0.001	0.001
Na ₂ SO ₄	0.001	0.018
Aluminum Nitrate (9 H ₂ O)	0.250	0.750
Sodium Phosphate (12 H ₂ O)	0.002	0.000

4.4.2 Experimental Design and Batching

The mixtures were designed to achieve high waste loading while resulting in little or no bleed water and a minimum 28 day compressive strength of 500 psi. The standard water to powder ratio was 0.60, with some exceptions. The test matrix of mixtures is shown in Table 4.16. Two of the three fly ashes were blended with low aluminate solutions. The slag was used as a partial replacement for fly ash, comprising 15 wt% of the aluminosilicate powder, and each of the three fly ashes was tested as a blend with slag. A slag and low aluminate simulant mixture was completed; however the resulting mixture was deemed unstable in air. Therefore, mixes with the high aluminate simulant were mixed with both slag and fly ash to minimize the reactivity in air. Mixing was completed using a shear mixer with a four-blade vane style attachment. The solution was added to the mixing vessel and the initial mixer was set at 300 rpm. The powder was added to the vessel over approximately 1 minute. The speed of the mixer was increased to a range of 600-700 rpm, depending on the consistency of the mixture. Mixing was completed for a total of approximately 3 minutes, after visually confirming that the solids had been completely incorporated with the liquid portion.

Table 4.16. Test Matrix for Geopolymer Mixtures with the Low Aluminate Waste Stream 1.

	Low Aluminate (4.0 M)	Water to Powder Ratio
Class C (Boral)	x	0.70
Class F (Big Brown Raw)	x	0.70
Class C (Boral)	x	0.60
Class F (Big Brown Raw)	x	0.60
Slag	x	0.60
Class C / Slag (85/15)	x	0.60
Class F (BBR) / Slag (85/15)	x	0.60
Class F (Belews) / Slag (85/15)	x	0.60

4.4.3 Measurement of Fresh and Cured Properties

Fresh state testing for the gel time of the mixture under static conditions was completed on specimens placed in 1 mL vials. The vials were filled approximately 2/3 full and one vial was inverted every 10 minutes until the mixture no longer flowed out of the vial when turned upside down. The time to this point was recorded as the mixture's gel time. The other specimens made included bleed water specimens and compressive strength cylinders. The bleed water specimens were cast in 125 mL bottles with screw-top lids. The specimen was weighed and the lid attached. The specimens were placed in a temperature-controlled 23° C room until the bleed water was measured at 24 hours. To measure the bleed water, water remaining on the surface of the specimen after 24 hours was pipetted off and weighed. The water was returned to the specimen and the specimen was re-sealed. Compressive strength specimens were cast in 50 mm x 100 mm (2" x 4") plastic cylinder molds. The cylinders were filled to the top, and sealed with the snap-on lids. The cylinders were stored in a temperature-controlled 23 °C room until they were demolded and tested for compressive strength at 28 days. In order to test for compressive strength, the cylinders were capped with sulfur compound such that any surface unevenness was eliminated.

The gel time, normalized bleed water, and compressive strength for all mixtures are presented in Table 4.17. The gel time is the only fresh state property measured for these mixtures. The Big Brown Raw Class F fly ash mixtures without slag had the longest gel times at approximately one hour, while the slag, Class C fly ash, and blended slag/fly ash mixtures had short gel times of 10-20 minutes. The Belews Creek/slag gel time using low aluminate simulant had an intermediate gel time of 30 minutes. The results show that an increased calcium content in the cementitious materials resulted in decreased gel times. The bleed water masses for each specimen are normalized to a 100 g of geopolymer, since the bleed specimen size varied from batch to batch. The systems containing slag and/or Class C fly ash had little or no bleed at 24 hours.

Table 4.17. Gel time, normalized bleed water and compressive strength for all geopolymer mixtures tested.

	Water to Powder Ratio	Gel Time (min)	Bleed Water (g)	Compressive Strength (psi)
Class C (Boral)	0.70	20	0.1	294
Class F (Big Brown Raw)	0.70	50	2.0	558
Class C (Boral)	0.60	20	none	421
Class F (Big Brown Raw)	0.60	40	1.8	818
Slag	0.60		none	1935
Class C / Slag (85/15)	0.60	10	none	2658
Class F (BBR) / Slag (85/15)	0.60	10	none	4602
Class F (Belews) / Slag (85/15)	0.60	30	0.6	1094

Compressive strength testing results are presented in Table 4.17. Only select mixtures resulted in compressive strength values at 28 days that exceeded those required by the project parameters. The Class C fly ash mix did not exceed the strength requirements. The mean compressive strength of the waste form shall be determined by testing representative non-radioactive samples. The compressive strength shall be at least 3.45E6 Pa when tested in accordance with ASTM C39/C39M-99 or an equivalent testing method.²¹ The remaining mixtures with low aluminat simulant all exceeded 500 psi (3.45E6 Pa) at 28 days and were considered as good contenders for waste immobilization in geopolymers.

4.4.4 Scanning Electron Microscopy

SEM analyses were performed on specimens in which curing was stopped using ethanol at 14 days. After 14 days of curing, the bleed specimen was cut open using a concrete saw with cutting oil lubricant. A portion of the specimen was cut that was approximately 50 mm in diameter and 20mm thick. This portion was placed in a beaker filled with an excess volume of ethanol. The specimen was allowed to soak for approximately 48 hours, removed, dried with paper towels, and placed in a vacuum desiccator for further drying. The specimen was cut down to SEM samples of approximately 10 mm x 10 mm x 1 mm thick. These specimens were dried in the vacuum desiccator for 24 hours prior to vacuum impregnation. Vacuum impregnation was completed using the following method. Molds measuring approximately 32 mm in diameter and 25 mm high were wiped with mold release oil on the sides and joints. The specimen was placed face-up in the mold, and the mold was placed in the vacuum impregnation unit. The unit was equipped with a turntable, such that multiple specimens could be made at once. The specimen was vacuumed to 25 mm Hg and held for approximately 10 minutes while the epoxy was mixed. The epoxy used in this process was manufactured by Logitech and was a two-part epoxy for which the resin/ hardener ratio was 4:1 by mass. The epoxy was dispensed into a cup at the center of the vacuum chamber while still under vacuum and allowed to rest until air bubbles introduced during the dispensing process were allowed to rise to the surface and fully escape the epoxy. Next, each specimen mold was filled with epoxy to approximately 6 mm by tilting the paper cup over each mold. The specimens were allowed to rest for 30 minutes under vacuum with the epoxy. The vacuum was slowly released, and the specimens were allowed to rest for another 30 minutes. Finally, the specimens were cured for a minimum of 24 hours at room temperature before grinding and polishing.

Grinding was completed by hand with SiC papers and no lubricant using the following grades of SiC paper: #60, 180, 400, 600, and 1200. The coarsest paper, #60, was used to expose approximately 70% of the area of the geopolymer paste surface. The remaining papers were used to remove material at decreasing rates. Once the grinding was completed, the specimens were polished using an automated polishing head with 5 lbf of force to the polishing cloth and approximately 60-80 rpm. Twill polishing cloths mounted on a platen diamond paste applied. The diamond pastes included 6 μm , 3 μm , 1 μm , and 1/4 μm . In many instances, the specimens were submerged in a beaker of ethanol and placed in the ultrasonic cleaner for approximately 10 seconds before moving to a finer diamond paste in order to dislodge any remaining diamond paste. The specimens were coated with carbon to approximately 20-25 nm thick using the brass substrate method³⁴ prior to analysis in the SEM.

SEM microanalyses were completed on the geopolymer pastes that exceeded the 500 psi compressive strength requirement. The images were assessed for the presence of unreacted particles (circular for fly ash and angular for slag), for general integrity i.e. cracking, and for the apparent density of the reaction product. X-ray mapping proved inconclusive for determining composition of the reaction product, due to widespread presence of elements in the reaction product. Unreacted particles were identified with x-ray mapping. Figure 4.14 is a micrograph of the Big Brown Raw fly ash mixed with low aluminate simulant solution after 14 days of curing. Minimal unreacted fly ash (bright circle-shaped particles), was observed in the image, while reaction products appeared to be of varying composition due to the contrast between different areas of the specimen.

Figure 4.15 is a backscattered electron image of the Big Brown Raw fly ash and slag blend, mixed with low aluminate simulant. Unreacted spherical fly ash particles were visible as light gray and white circles, while reaction product surrounded the particles. The microstructure of the geopolymer appeared to be somewhat uncompacted, with a porous appearance. Some cracking was apparent, but it was not widespread. This figure contrasts with the Class C/slag and Belews Creek/ slag blends mixed with low aluminate simulant mixtures (Figure 4.16 and Figure 4.17). The Class C fly ash and slag blend resulted in greater reaction product than the two class F fly ashes. The Belews Creek fly ash/slag blend geopolymer appeared to have the least reaction product, given the many unreacted particles present in the image, which appear as circular particles with smooth textures. Figure 4.14 through Figure 4.17 have the same field width of approximate 600 micrometers, to facilitate comparison.

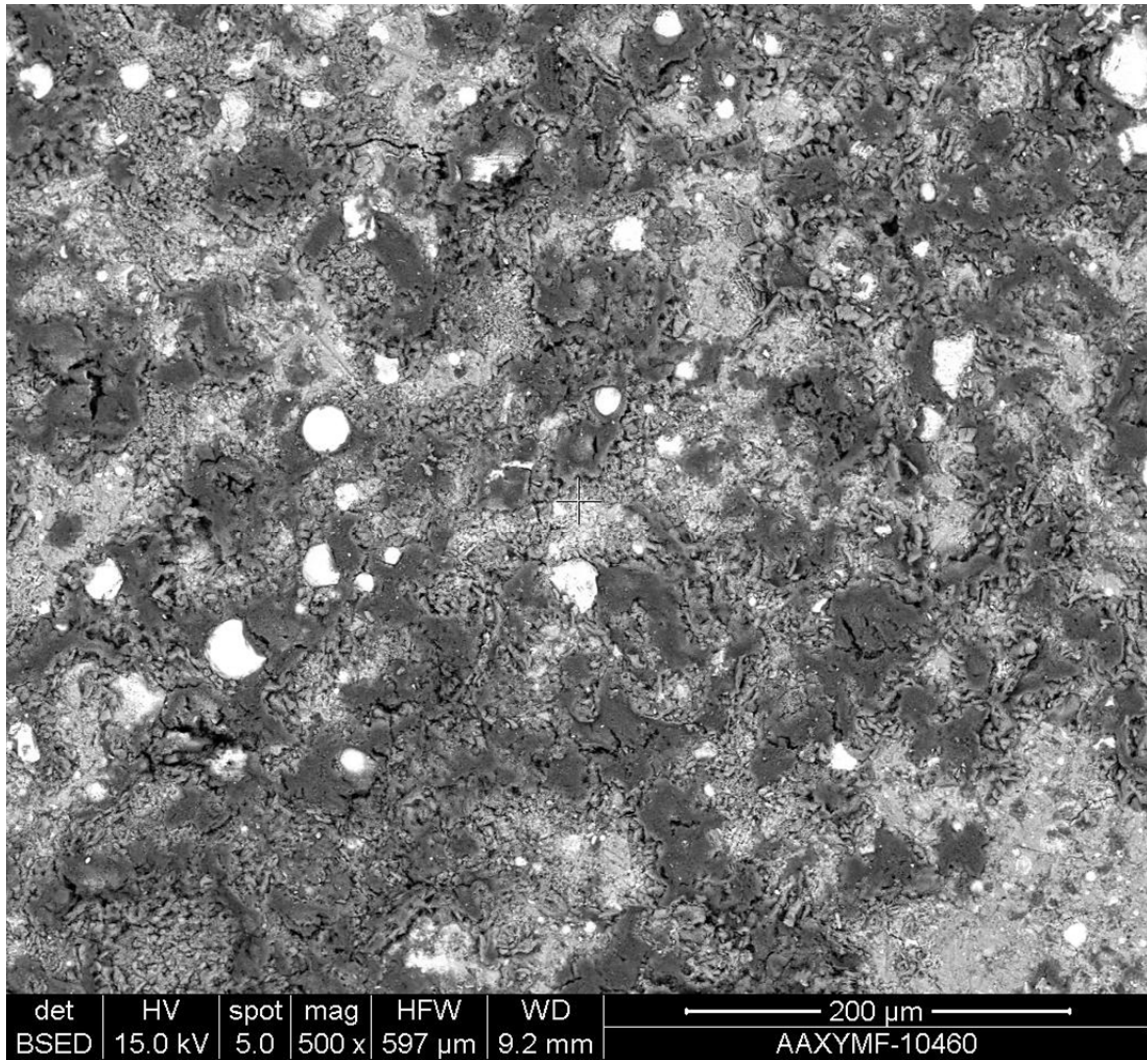


Figure 4.14. Low aluminat simulant and Big Brown Raw fly ash geopolymer paste after 14 days of curing at room temperature.

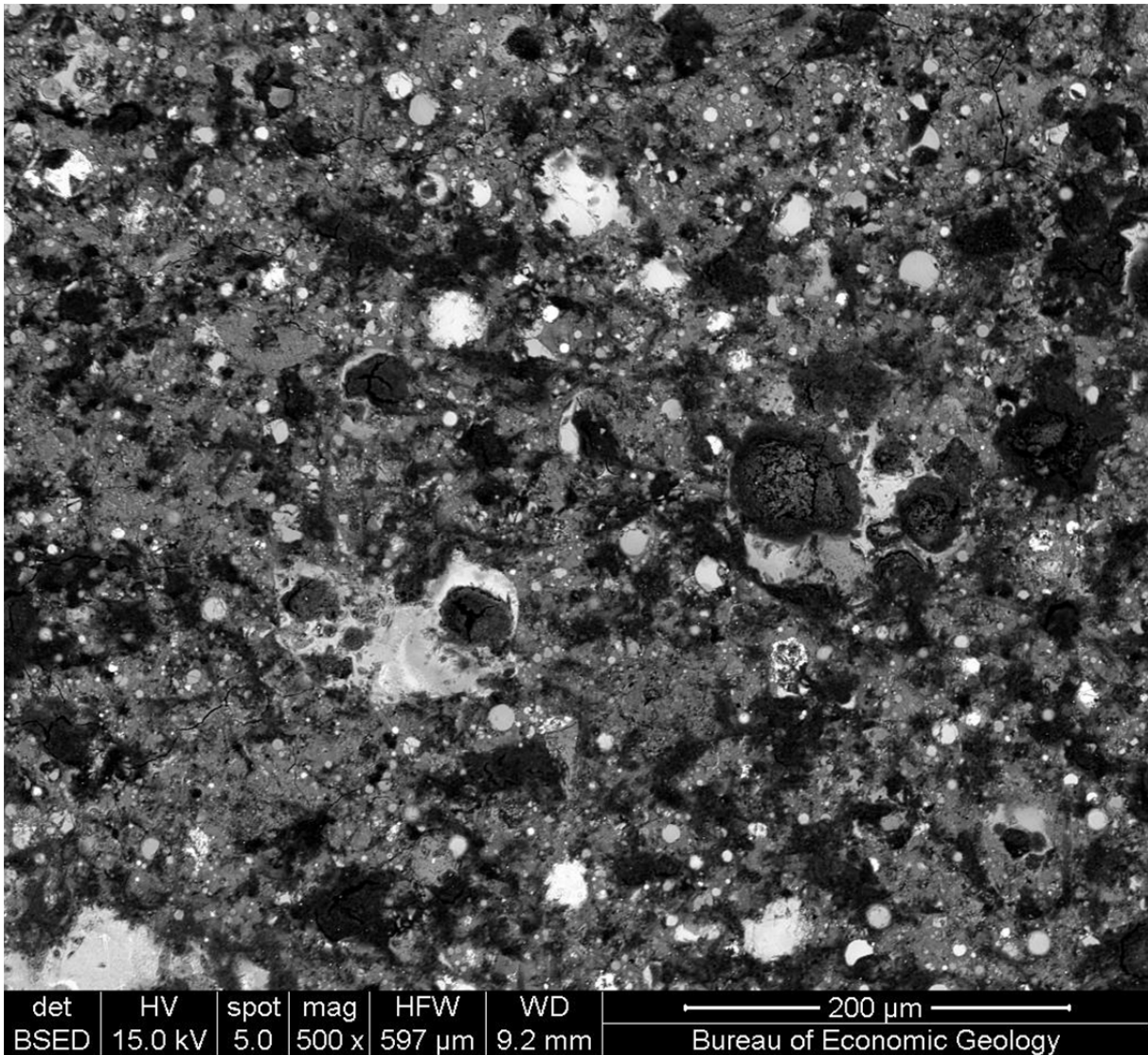


Figure 4.15. Low aluminated simulant mixed with big brown raw and slag geopolymer pastes after 14 days of curing at room temperature.

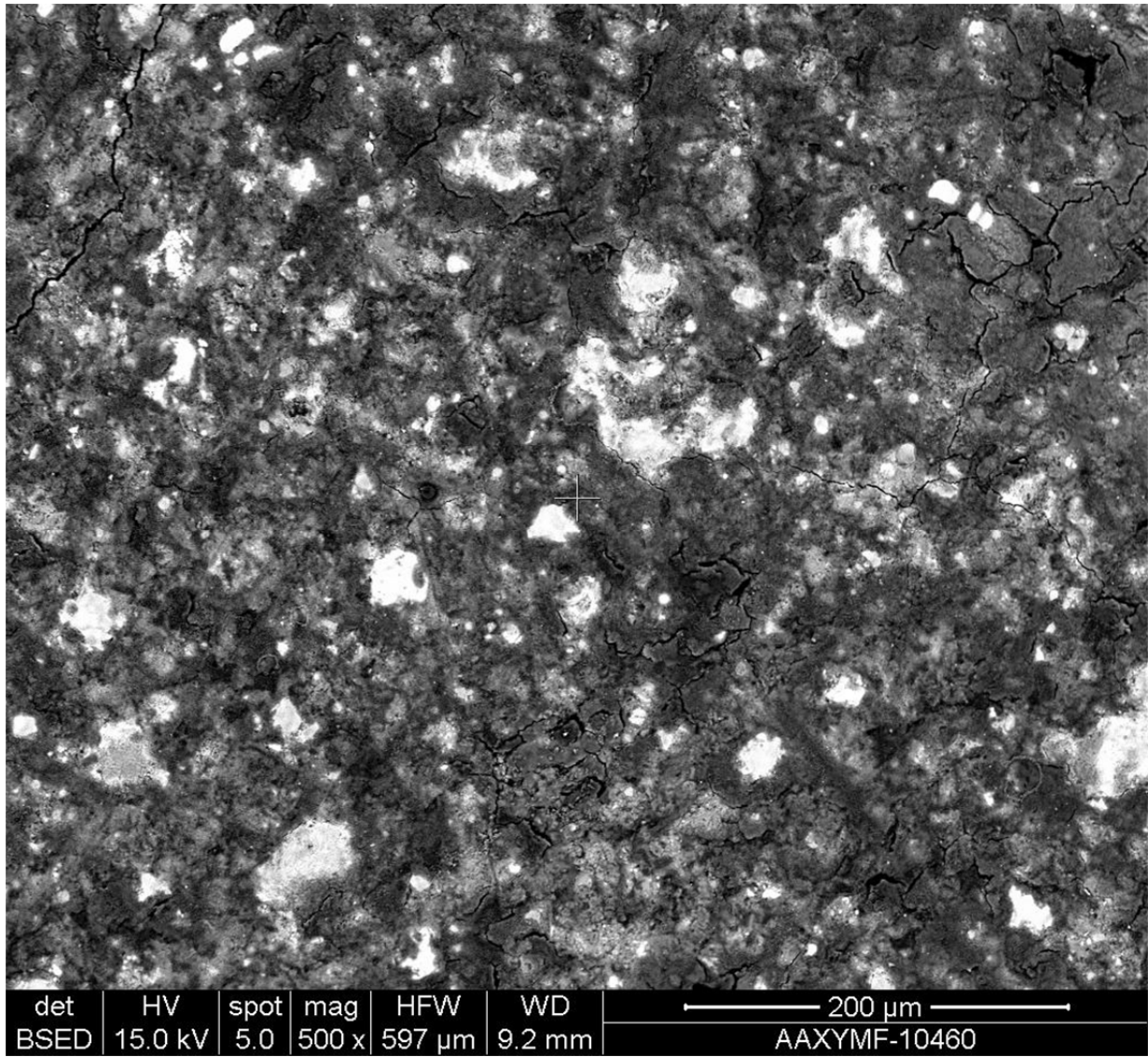


Figure 4.16. Low aluminate simulant mixed with Class C fly ash and slag geopolymer after 14 days of curing at room temperature

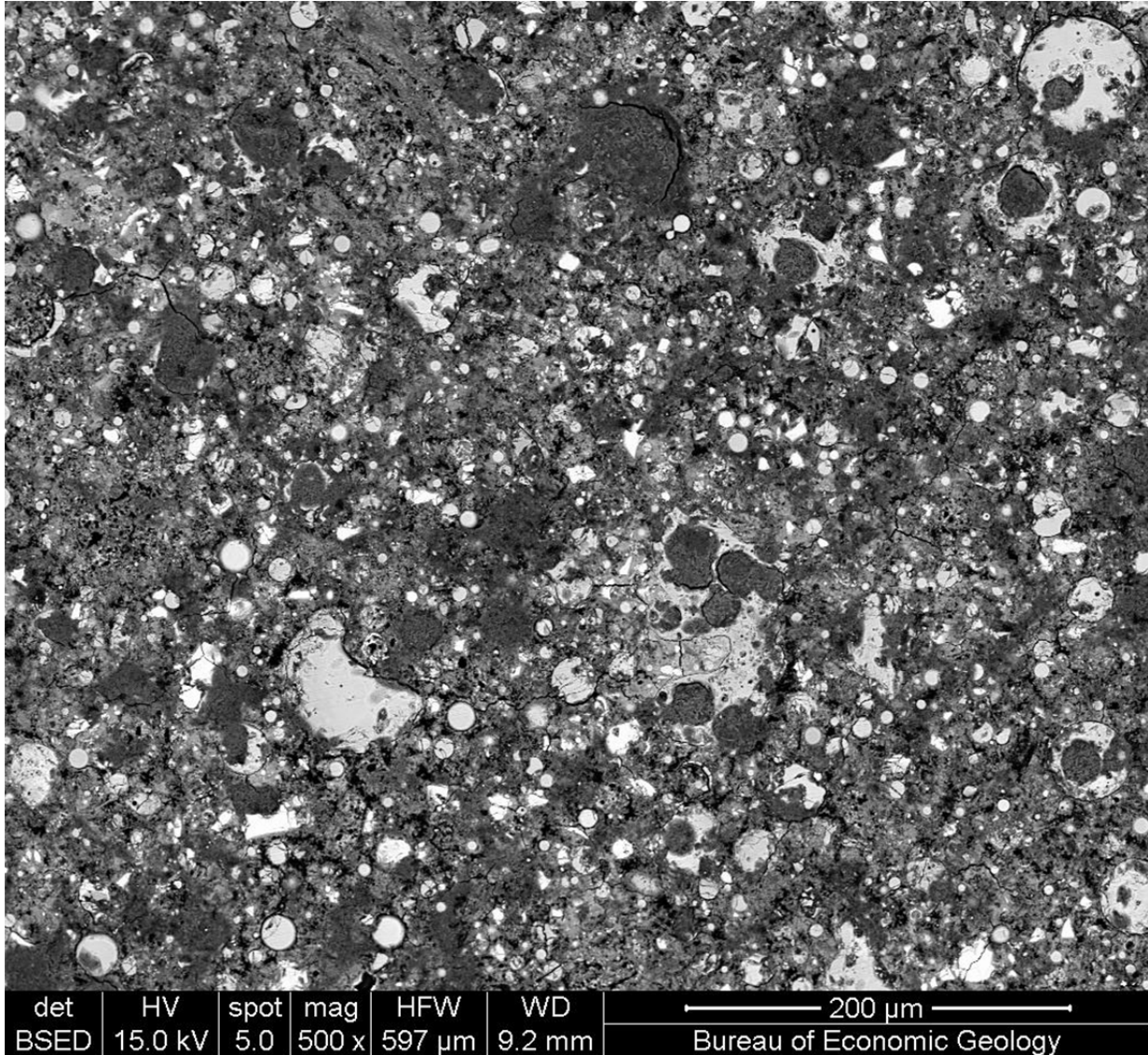


Figure 4.17. Low aluminate simulant mixed with Belevs Creek fly ash and slag, geopolymer paste after 14 days of curing at room temperature

4.4.5 Heat Generation

The heat flow and integrated heat output for two of the blended mixes were measured using an isothermal calorimeter operated at 25 °C as previously described.³⁵ The first mix measured contained 85 wt % Big Brown Raw Class F Fly Ash and 15 wt % slag with the low aluminate simulant at a 0.60 water to powder ratio (Figure 4.18). The second mix contained 85 wt % Class C Fly Ash and 15 wt % slag with the low aluminate simulant (0.60 water to powder ratio) shown in Figure 4.19. The amount of heat generated is significant and approaches or exceeds that observed with Saltstone mixes under similar conditions.³⁶

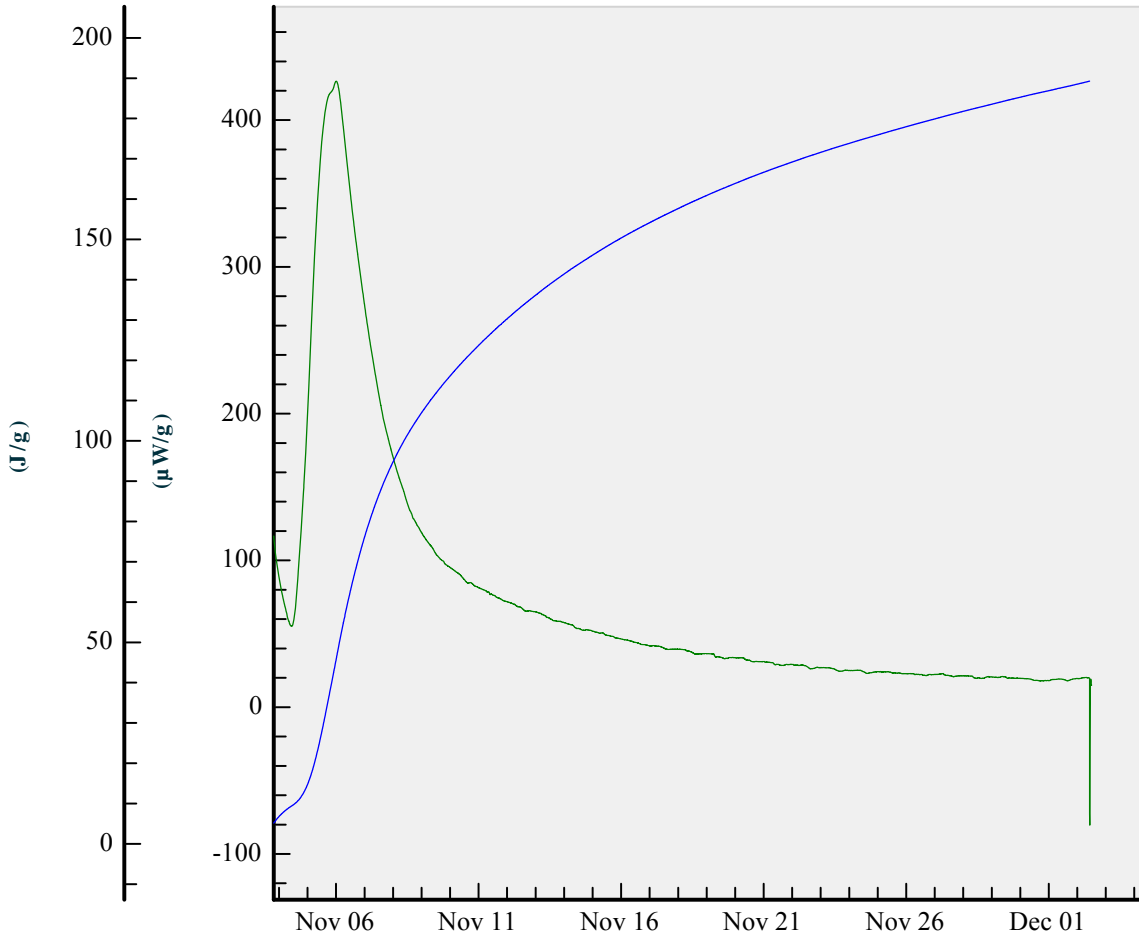


Figure 4.18. Isothermal calorimetry output for a mix of low aluminate waste stream # 1 with a premix composed of 85 wt % Big Brown Raw Class F fly ash and 15 wt % slag.

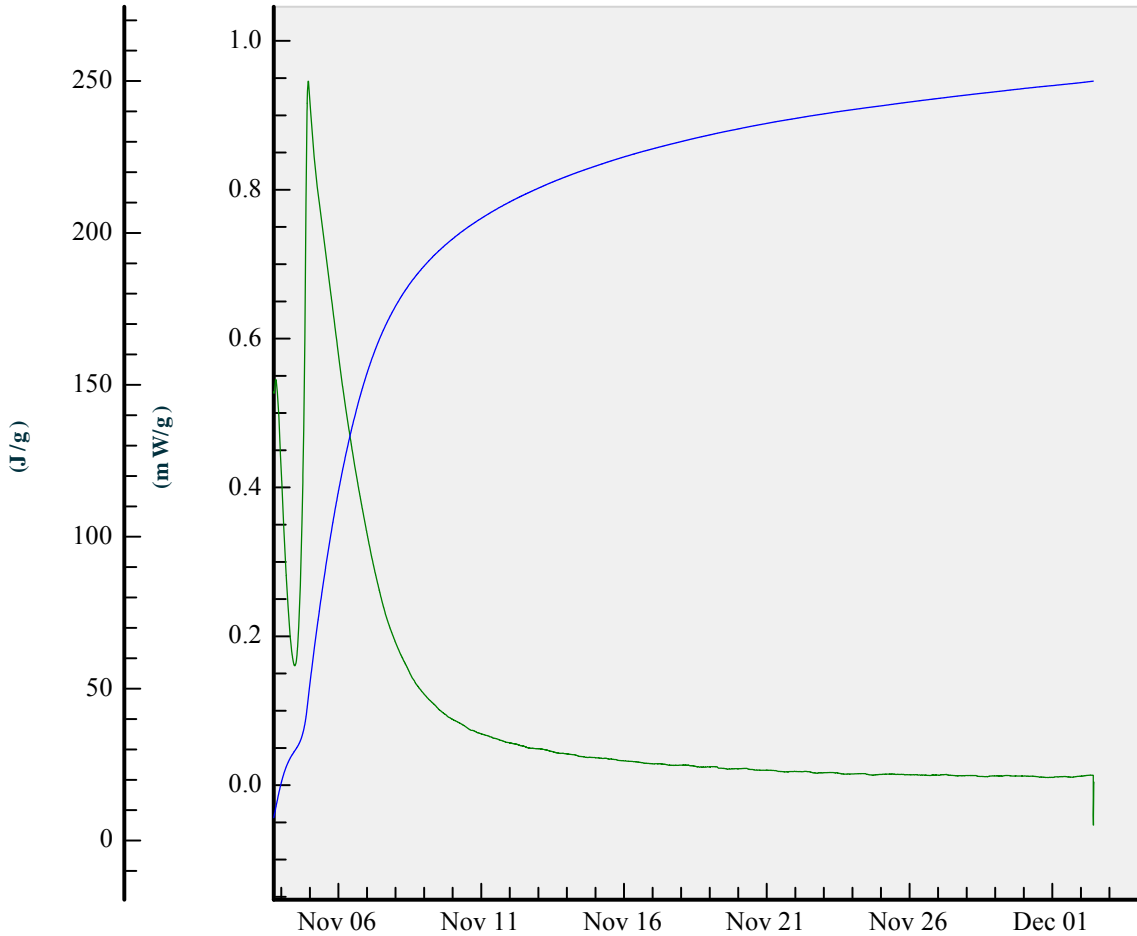


Figure 4.19. Isothermal calorimetry output for a mix of the low aluminate waste stream # 1 with a premix composed of 85 wt % Class C fly ash and 15 wt % slag.

4.4.6 Volume and Mass Factors

Waste volume and mass factors will be close to those of the Saltstone/Cast Stone mixes discussed in section 4.5. However, they are slightly different due to the higher concentrations of NaOH in the waste stream # 1 after aluminum dissolution vs. waste stream # 2 which has reduced NaOH due to recovery.

Table 4.18. Volume and mass fractions of geopolymer waste form.

By Volume			
Volume of Waste (L)	% Loading (in grout)	Volume of Grout (L)	Volume Factor
1.0	40	1.6	1.6
By Mass			
Mass of 1 L of Waste	Mass of Grout	Mass Factor	
1100	2700	2.5	

4.4.7 Future Work

Retention of I and Re will be measured as discussed in Section 4.5. Blast furnace slag was added to the mixes to provide a reductant that will reduce pertechnetate to Tc⁴⁺. A separate getter may be required for retention of I-129.

Initial mixes revealed compressive strengths that are less than 500 psi for the high aluminate mixes. Additional formulation work will therefore be performed with the high aluminate mixes to achieve higher compressive strengths. Formulation development will also need to be performed on waste streams # 2. Geopolymer formulations made with fly ashes available in the Hanford area must also be evaluated since the composition can vary greatly between fly ashes.

4.5 Saltstone/Cast Stone Waste Form

A cementitious waste form has the advantage that the process is performed at ambient conditions and consequently, has lower power consumption than glass production without the need for a complex off-gas treatment system. Saltstone was developed for the low level waste stream generated at SRS while Cast Stone was developed as a treatment option for Hanford LAW. This method of waste treatment has been deployed and is currently operating at SRS with the grout waste form disposed of in covered vaults which eventually will be completely covered. The current grout formulation (mix design) for Saltstone (which is essentially equivalent to the Cast Stone formulation) was tested with the two waste streams. For this initial testing, a water to premix ration of 0.60 was selected.

4.5.1 Saltstone Formulation

The cementitious materials for these mixes (Table 4.19) were obtained from the SPF. Table 4.19 also contains the weight percent contribution of each material used to make the premix. The fly ash used in this study was a material that had been thermally treated by the Vendor to remove most of the carbon and ammonia (carbon burnout or CBO fly ash).

Table 4.19 Cementitious Materials Used in Saltstone/Cast Stone Waste Form.

Material	Category	Vendor	Premix wt %
Portland Cement	Type II	Holcim	10
Blast Furnace Slag	Class 1	Holcim	45
Fly Ash	Class F	Holcim	45

The isothermal calorimetric data for these two mixes at 25 °C are shown in Figure 4.20. The high aluminate mix has an induction period which can account for the higher set time for this mix compared to the low aluminate mix. The high aluminate mix also produces more heat (normalized to the mass of cementitious materials) than the low aluminate mix and produces a waste form with higher Young's modulus and lower permeability.^{35,36}

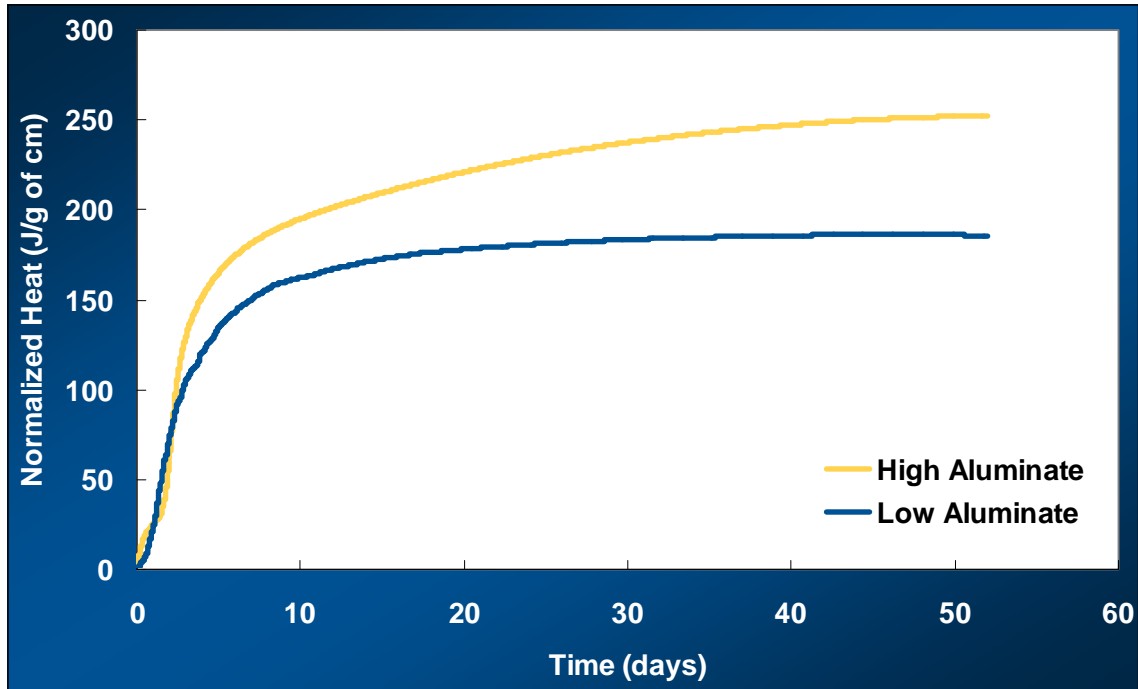


Figure 4.20. Normalized heat production (J/g of cm) for low and high aluminate mixes at 25 °C.

4.5.2 Performance Properties of Saltstone

Table 4.20 lists the processing properties for the low and high aluminate simulated waste streams. No effort was made to extend the gel time by addition of a set retarder. The three day set time is typical for waste streams containing higher aluminate levels.³⁶ The yield stress and consistency are lower for the higher aluminate mixes as previously determined.³⁶

Table 4.20. Processing properties for simulated low and high aluminate waste streams.

Properties	Low Aluminate	High Aluminate
Gel Time	10 minutes	20 minutes
Set Time	1 day	3 days
Bleed Volume	None	None
Density	1.67 g/mL	1.71 g/mL
Yield Stress	7.1 Pa	2.0 Pa
Consistency	0.08 Pa·s (80 cP)	0.02 Pa·s (20 cP)

The value of the dynamic Young's modulus (E) provides evidence on the strength and elasticity of the cured grout waste forms and on the performance properties in general. The values of E for the samples cured at 20 °C are between 7 and 8 GPa. However, Figure 4.21 shows that E is sensitive to the curing temperature and that the higher aluminate mix is more sensitive than the low aluminate mix. Curing temperature can play a role in the final performance properties depending on the size of the container, rate of filling, and the environmental conditions under which the pour is conducted.³⁷

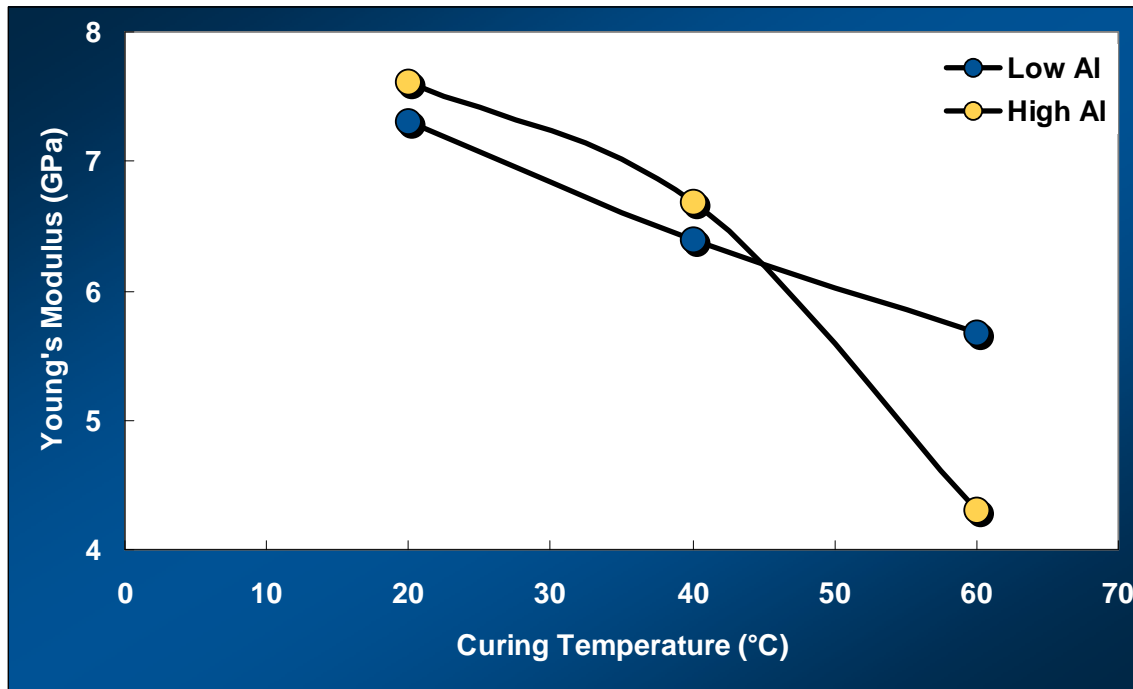


Figure 4.21. Dependence of Young's modulus on the curing temperature of the grouts.

4.5.3 Radionuclide Retention

The retention of I-129 and Tc-99 within the grout waste form is important for the PA of the IDF. Therefore, a technique was developed which will allow for the measurement of the retention of these species within the grout waste form through measurement of the composition of the pore solution. Non-radioactive iodide and rhenium (as a surrogate for technetium) were introduced into the simulated waste form.

Pore solution can be separated from the cured grout samples using the Unsaturated Flow Apparatus (UFA) centrifuge system³⁸ (Figure 4.22). The hydraulic conductivity can be calculated from the flow of liquid through the porous medium over time.³⁹ Using the UFA system the pore solution can be removed by two methods: (1) centrifugation only and (2) by centrifugation with continuous replenishment and flow of water through the system (as normally done when measuring liquid permeability of grouts).³⁹ The second method maintains permeant flow during centrifugation. For these samples, the permeant was fed gravitationally to the sample which promotes and maintains saturation of the samples.

Figure 4.23 plots the total sodium concentration of the pore solution as a function of time with continuous replenishment of the pore solution by water during centrifugation. The sodium ion concentration is relatively constant for the first 5 to 10 grams collected. After that the water begins to mix with the pore solution and the total sodium ion concentration is reduced. For this sample there are ~ 22 grams total of pore solution in the sample. Therefore collection of the first 5 grams of pore solution will provide a representative sample for chemical analysis. The retention of I and Re in the sample is calculated from the concentration in original waste stream and the concentration in the collected pore solutions.

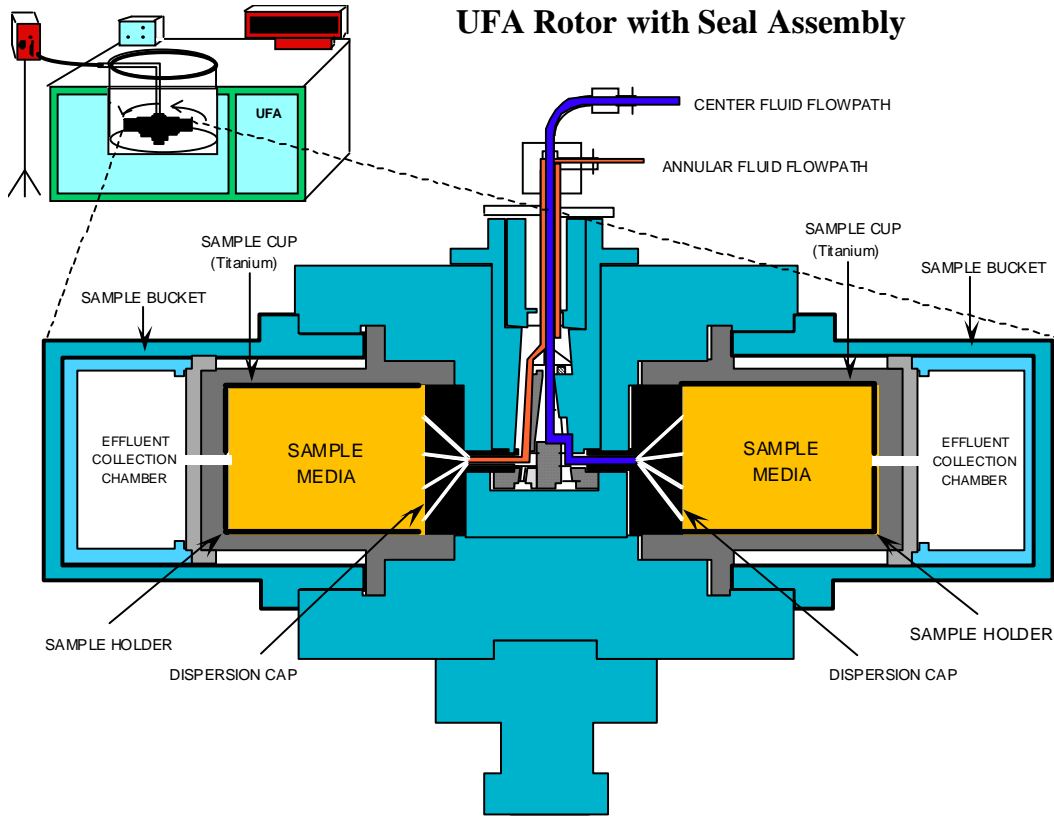


Figure 4.22. The UFA centrifuge system for measuring permeability and capturing pore solution.

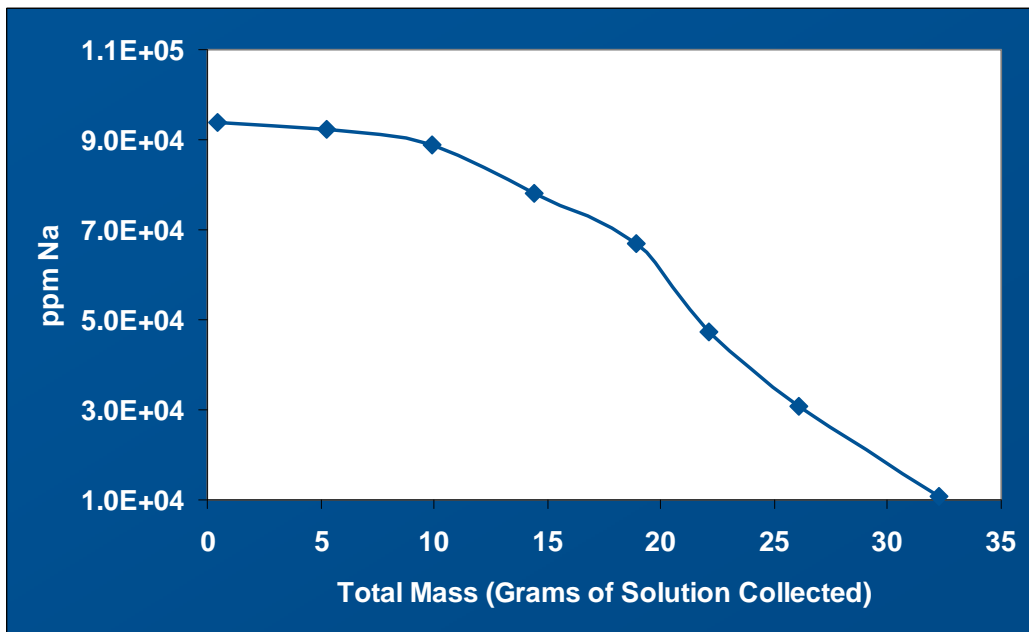


Figure 4.23. Total Na ion concentration (ppm) for each sample taken as a function of the total amount of solution collected.

A feasibility study was performed in which the Re-doped simulants were mixed with premix at a 0.60 water to premix ratio and allowed to cure. For this test, 2 inch diameter cured grout cylinders were placed in the centrifuge and the pore solution collected after centrifugation at 4000 rpm for 2 hours. The Re concentrations in the pore solutions were significantly reduced relative to the original concentrations in the low and high simulants (Table 4.21). Therefore, the method is applicable to a determination of retention of Re, I and any other soluble species of concern. The volume and mass factors for the mixes are provided in Table 4.22.

Table 4.21. Re Retention in the Low and High Aluminate Mixes

	Re in Simulant (ppm)	Re in Pore Solution (ppm)	Re Retention (%)
Low Aluminate	3.07E+05	3.60E+03	98.8
High Aluminate	2.99E+05	6.88E+03	97.7

Table 4.22. Waste Loadings and Associated Volume and Mass Factors for the Mixes.

By Volume			
Volume of Waste (L)	% Loading (in grout)	Volume of Grout (L)	Volume Factor
1.0	40.1	1.58 – 1.61	1.58 – 1.61
By Mass			
Mass of 1 L of Waste	Mass of Grout	Mass Factor	
1086 – 1147	2680 – 2705	2.34 – 2.49	

4.5.4 Future Work

The Saltstone/Cast Stone samples need to be tested for compressive strength to ensure they are within the required limits for WTP. In addition, further correlations between the grout formulation and performance properties needs to be evaluated to ensure that all waste streams immobilized as a cementitious waste form meets the contract requirements.

5.0 Conclusions and Path Forward

Five waste forms were evaluated for immobilization of LAW at Hanford after the sodium recovery process. The waste forms considered for these two waste streams include low temperature processes (Saltstone/Cast stone and geopolymers), intermediate temperature processes (steam reforming and phosphate glasses) and high temperature processes (vitrification). These immobilization methods and the waste forms produced were evaluated for (1) compliance with the Performance Assessment (PA) requirements for disposal at the IDF, (2) waste form volume (waste loading), and (3) compatibility with the tank farms and systems.

The iron phosphate glasses tested using the product consistency test had normalized release rates lower than the waste form requirements although the CCC glasses had higher release rates than the quenched glasses. However, the waste form failed to meet the vapor hydration test criteria listed in the WTP contract. In addition, the waste loading in the phosphate glasses were not as high as other candidate waste forms. Vitrification of HLW waste as borosilicate glass is a proven process; however the HLW and LAW streams at Hanford can vary significantly from waste currently being immobilized. The ccc glasses show lower release rates for B and Na than the quenched glasses and all glasses meet the acceptance criterion of < 4 g/L. Glass samples spiked with Re_2O_7 also passed the PCT test. However, further vapor hydration testing must be performed since all the samples cracked and the test could not be performed. The waste loading of the iron phosphate and borosilicate glasses are approximately 20 and 25% respectively.

The steam reforming process produced the predicted waste form for both the high and low aluminate waste streams. The predicted waste loadings for the monolithic samples is approximately 39%, which is higher than the glass waste forms; however, at the time of this report, no monolithic samples were made and therefore compliance with the PA cannot be determined.

The waste loading in the geopolymer is approximately 40% but can vary with the sodium hydroxide content in the waste stream. Initial geopolymer mixes revealed compressive strengths that are greater than 500 psi for the low aluminate mixes and less than 500 psi for the high aluminate mixes. Further work testing needs to be performed to formulate a geopolymer waste form made using a high aluminate salt solution.

A cementitious waste form has the advantage that the process is performed at ambient conditions and is a proven process currently in use for LAW disposal. The Saltstone/Cast Stone formulated using low and high aluminate salt solutions retained at least 97% of the Re that was added to the mix as a dopant. While this data is promising, additional leaching testing must be performed to show compliance with the PA. Compressive strength tests must also be performed on the Cast Stone monoliths to verify PA compliance.

Based on testing performed for this report, the borosilicate glass and Cast Stone are the recommended waste forms for further testing. Both are proven technologies for radioactive waste disposal and the initial testing using simulated Hanford LAW waste shows compliance with the PA. Both are resistant to leaching and have greater than 25% waste loading.

6.0 Acknowledgements

The authors would like to recognize the contributions of: David Best, Paul Burket, Gene Daniels, and Vickie Williams at SRNL, David Windgard and Clemson University for SEM micrographs, MO-SCI Corporation and PNNL for glass formulation and testing, and the University of Texas at Austin for geopolymer formulation and testing.

7.0 REFERENCES

1. Allen, D.I., Raymond, R.E., Brouns, T.M., Choho, A.F., et al., "Recommendation for Supplemental Technologies for Hanford River Protection Project Potential Mission Acceleration," *Waste Management Symposia*, Tucson, AZ, 2003.
2. Kosson, D.S., Gallay, D.R., Pegg, I.L., Wymer, R.G., et al., "External Technical Review of System Planning for Low-Activity Waste Treatment at Hanford," 2008.
3. Harbour, J.R., "Waste Form Development for the Waste Stream Exiting Sodium Recovery after Aluminum Leaching of Hanford LAW," Savannah River National Laboratory, Aiken, SC, SRNL-RP-2010-00127, January 2010.
4. Snow, L., Lumetta, G., Fiskum, S., and Peterson, R., "Boehmite Actual Waste Dissolution Studies," *Separation Science and Technology*, **43**, 2900-16 (2008).
5. Peterson, R. and Fiskum, S. and Geeting, J. and Smith, H., et al., "Hanford Boehmite/Chromium Dissolution Data", Batelle-Pacific Northwest Division, PowerPoint Presentation.
6. McCabe, D.J., Peterson, R., Pike, J.A., and Wilmarth, W.R., "Aluminum and Chromium Leaching Workshop Paper," Savannah River National Laboratory, WSRC-STI-2007-00168, April 25, 2007.
7. Apps, J.A., Neil, J.M., and Jun, C.H., "Thermochemical Properties of Gibbsite, Bayerite, Boehmite, Diaspore, and the Aluminate Ion Between 0 and 350°C," Lawrence Berkeley Laboratory, NUREG/CR-5271, LBL-21482, 1989.
8. Reynolds, J.G. and Reynolds, D.A., "A Modern Interpretation of the Barney Diagram for Aluminum Solubility in Tank Waste," *Waste Management Symposia*, Phoenix, AZ, 2010.
9. Agnew, S.F., Reynolds, J.G., and Johnston, C.T., "Aluminum Solubility Model for Hanford Tank Waste Treatment," *Waste Management Symposia*, Phoenix, AZ, 2009.
10. Peterson, R., Russell, R., Sams, T., and Brasel, B., "Continuous Sludge Leaching", http://srnl.doe.gov/owp_techex09/denver_webcast/slides/04-5_Peterson.pdf, 2005.
11. Sresty, G., Brasel, B., and Peterson, R., "Advanced Remediation Technologies: Continuous Sludge Leaching", Parsons Infrastructure & Technology Group and Battelle Memorial Institute, PowerPoint Presentation, 2007.
12. "Briefing for DOE-EM Technical Expert Group: Near Tank Treatment System", Parsons, 2010.
13. Fountain, M.S. and Kurath, D.E. and Sevigny, G.J. and Poloski, A.P., et al., "Caustic Recycle from Hanford Tank Waste Using NaSICON Ceramic Membrane Salt Splitting Process," Pacific Northwest National Laboratory, PNNL-18216, Rev. 0, 2009.
14. Harbour, J.R., "Development of Hanford LAW Simulants for Waste Streams Resulting from Aluminum Leaching of HLW and Subsequent Sodium Recover (Near-Tank Treatment System)," Savannah River National Laboratory, SRNL-L3100-2010-00066, March 24, 2010.

15. Wilmarth, W.R., Hobbs, D.T., Averill, W.A., Fox, E.B., et al., "Review of Ceramatec's Caustic Recovery Technology," WSRC-STI-2007-00366 Rev. 0, 2007.
16. Balagopal, S. and Bhavaraju, S.V. and Clay, D.A. and Schatten, K.L., et al., "Recycling Caustic from LAW Stream using NaSICON Membrane Based Electrochemical Technology", PowerPoint Presentation, Ceramatec, Inc.
17. Geniesse, D., "A Process for Removal of Aluminum Oxides from Aqueous Media," PCT/US2008/076589, 2008.
18. Geniesse, D., "Test Program for Alumina Removal and Sodium Hydroxide Regeneration from Hanford Waste by Lithium Hydrotalcite Precipitation (Draft)", Prepared for Areva FS, Inc., 2009.
19. Duncan, J. and Huber, H., "Scouting Experiments for Alumina Reduction in WTP Feed", http://www.hanford.gov/files.cfm/CAL_DST_Lithium_Hydrotalcite.pdf.
20. Peterson, R., to J. R. Harbour, *Personal Communication* 2010.
21. "WTP Contract " Contract No. DE-AC27-01RV14136, Conformed Thru Modification No. M153,
22. "Standard Test Methods for Determining Chemical Durability of Nuclear, Hazardous, and Mixed Waste Glasses and Multiphase Glass Ceramics: The Product Consistency Test," ASTM International, ASTM C1285.
23. "Standard Test method for Measuring Waste Glass or Glass Ceramic Durability by Vapor Hydration Test," ASTM International, C 1663 - 09.
24. Jantzen, C.M., "Fluidized Bed Steam Reformer (FBSR) Monolith Formation," Savannah River National Laboratory.
25. Burket, P.R. and Daniel, W.E. and Jantzen, C.M. and Nash, C.A., et al., "Steam Reforming Technology Demonstration for the Destruction of Organics on Actual DOE Savannah River Site Tank 48H Waste," *Waste Management Symposia*, Phoenix, AZ, 2009.
26. Jantzen, C.M., Marra, J., and Mason, B., "MINCALC(TM)", Savannah River National Laboratory, 2004.
27. Crawford, C.L. and Burket, P.R. and Cozzi, A.D. and Daniel, W.E., et al., "Radioactive Demonstration of Mineralized Waste Forms Made from Hanford Waste Treatment Plant Secondary Waste (WTP-SW) By Fluidized Bed Steam Reformation (FBSR)," Savannah River National Laboratory, SRNL-STI-2011-00331 Revision 0, August 2011.
28. "Standard Specification for Coal Fly Ash and Raw or Calcined Natural Pozzolan for Use in Concrete," ASTM International, C618-08a, October 2008.
29. Bakharev, T., "Geopolymeric Materials Prepared Using Class F Fly Ash and Elevated Temperature Curing," *Cement and Concrete Research* **35**, 1224-32 (2005).
30. Fernández-Jiménez, A. and Palomo, A., "Characterization of Fly Ashes: Potential Reactivity as Alkaline Cements," *Fuel*, **82**, 2259-65 (2003).

31. Lloyd, R.R., "The Durability of Inorganic Polymer Cements"; Ph.D. Thesis. University of Melbourne, Melbourne, Australia, 2008.
32. Tailby, J. and MacKenzie, K.J.D., "Structure and Mechanical Properties of Aluminosilicate Geopolymer Composites with Portland Cement and its Constituent Materials," *Cement and Concrete Research*, **40**, 787-94 (2010).
33. Sofi, M., van Deventer, J.S.J., Mendis, P.A., and Lukey, G.C., "Engineering Properties of Inorganic Polymer Concretes (IPCs)," *Cement and Concrete Research*, **37**, 251-7 (2007).
34. Kerrick, D.M., "The Role of Carbon Film Thickness in Electron Microprobe Analysis," *American Mineralogist*, **58**, 920-5 (1973).
35. Harbour, J.R., Edwards, T.B., and Williams, V.J., "Performance Properties of Saltstone Produced Using SWPF Simulants," Savannah River National Laboratory, SRNL-STI-2009-00810, December 2009.
36. Harbour, J.R., Edwards, T.B., and Williams, V.J., "Key Factors That Influence the Performance Properties of ARP/MCU Saltstone Mixes," Savannah River National Laboratory, SRNL-STI-2009-00546, September 2009.
37. Harbour, J.R., Edwards, T.B., and Williams, V.J., "Impact of Time/Temperature Curing Conditions and Aluminate Concentration on Saltstone Properties," Savannah River National Laboratory, SRNL-STI-2009-00184, Rev. 0, 2009.
38. Harbour, J.R. and Williams, M.F., "Impact of Curing Temperature on the Saturated Liquid Permeability of Saltstone," Savannah River National Laboratory, SRNL-STI-2010-00745, February 2011.
39. "Standard Test Methods of Measurement of Hydraulic Conductivity of Saturated Porous Materials Using a Flexible Wall Permeameter," ASTM International, D5084-10, July 2010.